nature communications

Article

https://doi.org/10.1038/s41467-024-52436-w

ACL1-ROC4/5 complex reveals a common mechanism in rice response to brown planthopper infestation and drought

Received: 27 December 2023

Accepted: 5 September 2024

Published online: 16 September 2024

Check for updates

Zhihuan Tao[1,2], Lin Zhu[1,2], Haichao Li[1], Bo Sun[1,2], Xue Liu[3], Dayong Li[3], Wenli Hu[1], Shanshan Wang[1], Xuexia Miao[1] ✉ & Zhenying Shi[1] ✉

Brown planthopper (BPH) is the most destructive insect pest of rice. Drought is the most detrimental environmental stress. BPH infestation causes adaxial leaf-rolling and bulliform cells (BCs) shrinkage similar to drought. The BC-related *abaxially curled leaf1* (*ACL1*) gene negatively regulates BPH resistance and drought tolerance, with decreased cuticular wax in the gain-of-function mutant *ACL1-D*. *ACL1* shows an epidermis-specific expression. The TurboID system and multiple biochemical assays reveal that ACL1 interacts with the epidermal-characteristic rice outermost cell-specific (ROC) proteins. *ROC4* and *ROC5* positively regulate BPH resistance and drought tolerance through modulating cuticular wax and BCs, respectively. Overexpression of *ROC4* and *ROC5* both rescue *ACL1-D* mutant in various related phenotypes. ACL1 competes with ROC4/ROC5 in homo-dimer and hetero-dimer formation, and interacts with the repressive TOPLESS-related proteins. Altogether, we illustrate that ACL1–ROC4/5 complexes synergistically mediate drought tolerance and BPH resistance through regulating cuticular wax content and BC development in rice, a mechanism that might facilitate BPH-resistant breeding.

Plants are constantly challenged by diversebiotic and abiotic factors simultaneously. Brown planthopper (BPH) (*Nilaparvata lugens* Stål) is the most devastating insect pest specific to rice, causing yield losses of greater severity than other biotic stresses. In comparison with chemical insecticides and insect predators, endogenous genes provide longer-lasting resistance and an environmentally friendly means of BPH control. To date, 17 BPH resistance genes in rice have been cloned[1–11]. *Bph3* encodes a rice pattern recognition receptor that mediates the pattern-triggered immunity (PTI) response to BPH[4]. *Bph14* and *Bph26* encode nucleotide-binding-site-leucine-rich repeat family proteins, which recognize effectors from BPH and induce effector-triggered immunity (ETI)[1,3]. Elucidation of the underlying mechanism of BPH resistance genes has revealed a similar plant immune response against BPH and other pathogens[12–14]. However, rice might also have evolved distinct defense mechanisms to resist BPH based on its specific infestation characteristics and damaging features.

The typical symptom of BPH damage is withering of the plant, resulting in death, termed “hopperburn” when it occurs in the field, indicating a strong association with water loss. Consistently, BPH individuals aggregate at the base of stems and suck sap directly from the phloem. Therefore, blocking feeding through the deposition of callose (b-1, 3 glucan polymer) in the phloem cells provides resistance to BPH[1,15]. Generally, the open/close status and density of the stomata are the most crucial factors that influence water-loss efficiency. Transpiration accounts for 90% of total water loss under normal growth conditions. However, upon dehydration, the stomata close, and the cuticle controls non-stomatal water loss. Furthermore, the cuticle constitutes the initial natural barrier to biotic stresses[16]. Cuticular waxes comprise a mixture of hydrophobic very-long-chain fatty acids

[1]Key Laboratory of Plant Design, CAS Center for Excellence in Molecular Plant Sciences, Institute of Plant Physiology and Ecology, Chinese Academy of Sciences, Shanghai, China. [2]University of Chinese Academy of Sciences, Beijing, China. [3]National Engineering Research Center for Vegetables, Beijing Vegetable Research Center, Beijing Academy of Agriculture and Forestry Science, Beijing, P. R. China. ✉e-mail: xxm@cemps.ac.cn; zyshi@cemps.ac.cn

(VLCFA) and their derivatives[17]. Drought induces accumulation and compositional changes of waxes, and a greater wax content on the leaf surface improves drought tolerance[18–20]. Genes that influence wax content in rice, such as *Drought induced Wax Accumulation1* (*DWA1*), *Wax synthesis Regulatory1* (*OsWR1*), *OsGL1-6*, *Drought Hypersensitive* (*DHS*), and *Glossy1* (*GL1*) homologous gene *GL1-2* all affect water-loss efficiency and drought tolerance[20–24]. In addition, genes involved in VLCFA biosynthesis are up-regulated in small BPH (SBPH)-resistant rice plants[25], suggesting a possible connection between wax content and BPH resistance.

Drought is the most frequent abiotic stress that not only influences plant growth and development, but also reduces crop production and causes deterioration in global ecological environment[26]. Rice provides food for more than half of the world population, but its cultivation consumes a vast amount of water, and thus is especially vulnerable to drought throughout the growing season[27]. Therefore, novel strategies to improve rice productivity under limited water availability are critical for next-generation agriculture, which necessitates elucidation of the underlying mechanism of drought tolerance.

In rice, moderate leaf-rolling is beneficial to form a well-proportioned leaf area for photosynthesis[28] and may be strongly associated with drought tolerance[29]. Leaf-rolling is the most obvious and rapid response to drought and is caused by the rapid increase in transpiration rate that out-paces water absorption. Bulliform cells (BCs) are highly specialized epidermal parenchyma cells on the adaxial side of the leaf surface in graminaceous plants that lose water immediately upon drought stress, becoming smaller and enabling the leaf to roll inward to reduce further transpiration. Whether BC-associated leaf-rolling is associated with BPH resistance is of functional importance. Multiple genes that regulate BCs have been identified in rice. Overexpression of the *abaxially curled leaf1* (*ACL1*) gene and *zinc finger homeodomain class homeobox* (*OsZHD1*) gene increases the number and size of BCs, resulting in abaxially rolled leaves[30,31]. The *Arabidopsis* ACL1-homologous proteins, GLABRA2 (GL2)-interacting repressors1 (GIR1) and GIR2, regulate root hair formation as adapters of GL2, a homeodomain transcription factor function in epidermal cell fate determination, including trichome initiation and root hair formation[32,33]. GIR1 and GIR2 function in a repressor mechanism through interaction with the co-repressor TOPLESS[34]. *Rice outermost cell-specific gene5* (*ROC5*), *ROC8*, *SEMI-ROLLED LEAF1* (*SRL1*), and *leaf inclination2* (*LC2*) negatively regulate BC development, with their respective mutations enlarging BCs[35–38]. Overexpression of several genes, such as *lateral organ boundaries domain* (*LBD*) *gene OsLBD3-7*, *argonaute* gene *OsAGO7*, *narrow and rolled leaf1* (*NRL1*), *Rolling-leaf14* (*RL14*), *Homeodomain containing protein4* (*OsHB4*)[39–43], causes adaxially rolled leaves owing to a reduction in BC size and/or number. The *rolled and erect leaf2 (rel2) mutant exhibits an* increased number and reduced size of BCs in conjunction with adaxially rolled leaves[44]. Overexpression of *OsRRK1* results in a decrease in size and number of BCs and enhances BPH resistance, which, to date, is the only study that has investigated the relationship between leaf-rolling and BPH resistance[45].

Thus, BPH resistance might be closely associated with drought tolerance, but the underlying mechanism remains largely unclear. In this study, BC shrinkage occurred similarly under BPH infestation and drought. The BC-related *ACL1* gene negatively regulated BPH resistance and drought tolerance, and the cuticular wax content was greatly reduced in the *ACL1-D* mutant. The TurboID system identified several ROC proteins, and multiple biochemical assays confirmed the interaction between ACL1 and the ROCs. *ROC5* and *ROC4* positively regulated BPH resistance and drought tolerance. Specifically, *ROC4* and *ROC5* positively regulated wax content and leaf-rolling, respectively. Both *ROC5* and *ROC4* complemented the *ACL1-D* mutant as to the BPH resistance, drought tolerance, wax content, and leaf-rolling characters. Moreover, ACL1 competed with ROC4 and ROC5 in homo-dimer and hetero-dimer formation. Thus, *ACL1* synergistically regulated BPH resistance and drought tolerance in rice through repression of several ROC proteins.

Results

Response of rice plants to drought and BPH infestation

The typical symptom of BPH infestation of rice is leaf-rolling followed by withering of the entire plant. Leaf-rolling is also a general response of plants to drought. During normal growth, the wild-type (WT) rice plant ZH11 has flat leaves (Supplementary Fig. 1a). Upon BPH infestation for 6 days, ZH11 leaves rolled inward (adaxially) (Supplementary Fig. 1b). Similarly, the leaves rolled adaxially in response to drought (Supplementary Fig. 1c). Anatomical observation revealed that the BCs, whether adjacent to the primary vein or to the secondary veins, were distinctly shrunken compared with those under normal growth (Fig. 1a). Thus, the rice plants responded similarly to drought and BPH infestation, and leaf withering was initiated by shrinkage of the BCs.

Next, we examined the effect of co-treatment with drought and BPH infestation. Rice plants cultured in nutrition solution and co-treated with 20% PEG6000 and BPH infestation died earlier than those in the single treatments, and plants in the single treatments had a higher percentage of survival (Supplementary Fig. 2a–c).

To test whether drought-pretreated plants had increased BPH resistance, rice seedlings were treated first by withholding water for ~4 days until the plants began to wilt, and then re-watered for 2 days. After this initial treatment, these plants (termed "Pre-drought") were mostly shorter than the non-treated plants (Supplementary Fig. 3a). To compensate for the retarded growth, we planted a second batch of seedlings five days later (named "5d late") than the control. Under BPH infestation, the "5d late" plants died earlier than the control and "Pre-drought" plants (Supplementary Fig. 3b) and had lower survival rates (Supplementary Fig. 3c). The growth status and survival of the control and "Pre-drought" plants were similar till death (Supplementary Fig. 3c–e). Considering the delayed growth of the "Pre-drought" plants, and similar biomass of the "Pre-drought" and "5d late" plants, we concluded that the drought pretreatment increased the BPH resistance of the plants.

ACL1 negatively regulates drought tolerance and BPH resistance

ACL1 is associated with BC development[30]. To examine the tissue localization of *ACL1* transcripts, we generated pACL1:GUS-expressing plants, and the GUS signal was detected in almost all tissues examined, including the seedling, root, leaf sheath, leaf, culm, and spikelet (Supplementary Fig. 4). Specifically, in the cross-section of the root hair zone, the GUS signal was uniformly distributed (Fig. 1b), whereas in the cross-section of the root tip, the signal was much more concentrated and formed an "ACL1-GUS ring" of the epidermal cells (Fig. 1c). Furthermore, in the root, the GUS signal was also detected in the tiny trichomes (Supplementary Fig. 4b). Considering the trichome-specific expression of the *ACL1* homologous genes in tobacco[46] and tomato[47] respectively, we deduced that ACL1 might be an epidermal protein.

The expression of *ACL1* was responsive to drought and BPH infestation (Supplementary Fig. 5a, b). Various genetic materials of *ACL1* were constructed. A previously generated T-DNA insertion mutant that exhibited *ACL1* up-regulation (Supplementary Fig. 6a) and abaxially-rolled leaves (Supplementary Fig. 6b, c)[30] was re-named *ACL1-D*. *ACL1* overexpression plants were generated by transforming the ACL1–MYC fusion construct into NIP genetic background (Supplementary Fig. 6d, e), and exhibited abaxially rolled leaves (Supplementary Fig. 6f, g). Similarly, when the *Arabidopsis AtACL1* was overexpressed in rice (Supplementary Fig. 6h), the resulting AtACL1OE plants developed abaxially-rolled leaves (Supplementary Fig. 6i, j). Thus, the function of the *ACL1* gene in abaxial leaf-rolling was conserved between rice and *Arabidopsis*. In addition, we used CRISPR/Cas9 gene-editing technology and generated the ACL1KO line with a deletion of two nucleotides (Supplementary Fig. 7b). Furthermore, rice

https://doi.org/10.1038/s41467-024-52436-w

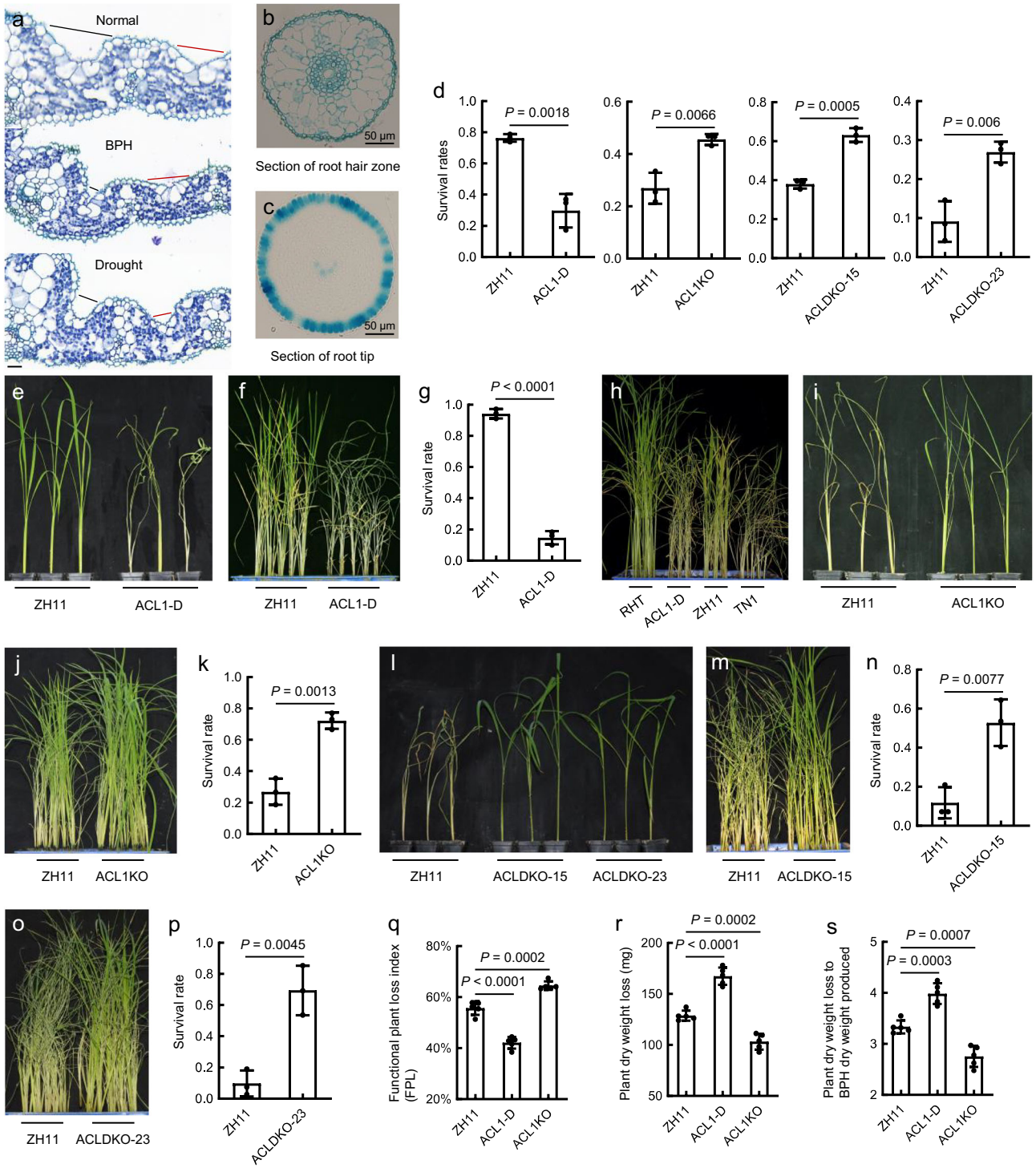

Fig. 1 | Leaf response to drought and BPH infestation, staining of pACL1:GUS roots, and genetic function of *ACL1* in drought tolerance and BPH resistance. **a** Transverse section of the leaf of ZH11 before treatment (normal), after BPH infestation for 6 days (BPH), and after drought (direct water cut-off) for 6 h (drought). Black lines and red ones indicate the bulliform cells adjacent to the main vein and the secondary vein, respectively. Bar is 20 μm. **b**, **c** GUS staining of the root hair zone (**b**) and root tip (**c**) of pACL1:GUS plants, respectively. Bars are 50 μm. **d** Survival of *ACL1-D*, ACL1KO, ACLDKO, and ZH11 plants under drought (direct water cut-off). **e**, **f** Phenotype of *ACL1-D* and WT plants after BPH infestation in an individual test (**e**) and small population test (**f**). **g** Survival of the plants in (**f**). **h** Phenotype of RHT, TN1, *ACL1-D*, and ZH11 plants to in response to BPH infestation. **i**, **j** Phenotype of ACL1KO and ZH11 plants after BPH infestation in an individual test (**i**) and small population test (**j**). **k** Survival of the plants in (**j**). **l**, **m**, **o** Phenotype of ZH11, ACLDKO-15, and ACLDKO-23 plants after BPH infestation in an individual test (**l**) and small population test (**m**, **o**). **n** Survival of the plants in (**m**). **p** Survival of the plants in (**o**). Data in (**d**), (**g**), (**k**), (**n**), and (**p**) are means ± SD ($n = 3$). **q** Functional plant loss index of the *ACL1-D*, ACL1KO, and ZH11 plants after BPH feeding. **r** Plant dry weight loss of *ACL1-D*, ACL1KO, and ZH11 plants after BPH feeding. **s** Plant dry weight loss to BPH dry weight produced of *ACL1-D*, ACL1KO, and ZH11 plants after BPH feeding. Data in (**q**), (**r**), and (**s**) are means ± SD ($n = 5$). The *P* values in (**d**), (**g**), (**k**), (**n**), and (**p**–**s**) were determined by a two-tailed unpaired Student's t-test. The experiments in (**a**–**c**) were repeated at least three times with similar results. Source data are provided as a Source Data file.

carries an *ACL1* homolog, *ACL2* (Supplementary Fig. 7a). We edited both *ACL1* and *ACL2* genes to generate the ACLDKO-15 and ACLDKO-23 lines (Supplementary Fig. 7c, d). The ACL1KO and ACLDKO plants all produced flat leaves (Supplementary Fig. 7e–h).

Two methods were used for the drought tolerance test, direct water cut-off and 20% PEG6000 treatment to simulate drought stress. In direct water cut-off, more *ACL1-D* plants died than WT plants (Supplementary Fig. 8), and thus had a lower survival rate (Fig. 1d). In contrast, fewer ACL1KO plants died (Supplementary Fig. 8), with a higher survival rate than the WT (Fig. 1d). Both ACLDKO lines withered later than WT plants (Supplementary Fig. 8) and had higher survival rates than the WT (Fig. 1d). Under 20% PEG6000 treatment, similar results were obtained (Supplementary Fig. 9). Taken together, these results indicated that *ACL1* negatively regulated drought tolerance. Also, both the AtACL1OE and ACL1-MYC plants withered earlier and had lower survival rates than their respective WT (Supplementary Figs. 10, 11). Thus, over-expression of *ACL1* in different genetic backgrounds and overexpression of *AtACL1* in rice increased the sensitivity to drought, further verifying the negative role of *ACL1* in drought response and the functional conservation of *ACL1* between rice and *Arabidopsis*.

Given that BPH infestation causes water loss, and that *ACL1* negatively regulates drought tolerance, we speculated that *ACL1* may regulate BPH resistance. Individual tests and small population tests were used to evaluate this hypothesis. In both types of assays, *ACL1-D* plants died earlier than ZH11 plants (Fig. 1e, f), and had a lower survival rate (Fig. 1g), indicating that *ACL1-D* plants were susceptible to BPH. When the BPH-resistant cultivar RHT, the BPH-susceptible cultivar TN1, *ACL1-D*, and ZH11 plants were compared in parallel, the susceptibility of *ACL1-D* plants was similar to that of TN1, with most *ACL1-D* and TN1 dying, ZH11 turning yellow, while RHT plants remaining green (Fig. 1h). The AtACL1OE plants were susceptible to BPH in both kinds of tests (Supplementary Fig. 12a, b), with a lower survival rate (Supplementary Fig. 12c). Also, the susceptibility of AtACL1OE plants to BPH was similar to that of TN1 (Supplementary Fig. 12d). The ACL1-MYC plants were more susceptible to BPH than NIP in both kinds of tests (Supplementary Fig. 12e, f) and had a lower survival rate (Supplementary Fig. 12g). The ACL1KO plants died later than the WT (Fig. 1i, j) and had a higher survival rate (Fig. 1k), indicating that ACL1KO plants had improved resistance to BPH. Similarly, ACLDKO-15 and ACLDKO-23 plants died later than the WT in both kinds of tests (Fig. 1l, m, o) and had higher survival rates (Fig. 1n, p). These results collectively indicated that *ACL1* negatively regulated BPH resistance.

Three kinds of physiological mechanisms are usually used by plants to invert herbivory insects, antibiosis, antixenosis, and tolerance[48]. To examine the mechanism of resistance to BPH in *ACL1-D* and ACL1KO plants, a BPH weight-gain test was performed, but no difference was observed (Supplementary Fig. 13a). Meanwhile, a choice test revealed no significant differences among the numbers of BPH settled on *ACL1-D*, ACL1KO, and ZH11 plants after infestation (Supplementary Fig. 13b). A tolerance test revealed that the functional plant loss (FPL) index of *ACL1-D* was lower than that of ZH11, whereas that of ACL1KO plants was higher (Fig. 1q). The plant dry-weight-loss and the plant dry-weight-loss to BPH dry-weight produced of the *ACL1-D* plants were higher than those of ZH11, whereas those of ACL1KO plants were lower (Fig. 1r, s). These results collectively indicated that neither antibiosis nor antixenosis were responsible for the BPH resistance of *ACL1-D* and ACL1KO plants, but the tolerance mechanism accounted.

Wax content is promoted in ACL1KO plants but decreased in *ACL1-D* plants

To explore the underlying mechanism of *ACL1* functioning, we conducted a mRNA-sequencing analysis of the *ACL1-D* and ZH11 plants. In the KEGG-pathway analysis, the fatty acid elongation pathway and the lipid metabolism pathway were distinctly enriched in the *ACL1-D* vs. ZH11 comparison (Supplementary Fig. 14), indicating that *ACL1* might influence wax content. Therefore, we examined the leaf surface of *ACL1-D*, ACL1KO, and ZH11 plants using a scanning electron microscope (SEM). The leaf surface of the *ACL1-D* plants was sparsely covered, whereas that of the ACL1KO plants was densely covered with wax crystals, including the unevenly distributed cuticular papillae (CP) (Fig. 2a–c). On the leaf sheath surface, wax crystals were denser in the ACL1KO while sparser in the *ACL1-D* plants (Fig. 2d–f). GC-MS revealed that waxes, especially C22–C30 VLCFA, were distinctly lowered in abundance in the *ACL1-D* plants, but were increased in abundance in the ACL1KO plants (Fig. 2g). Similarly, in both ACLDKO lines, the wax content was higher (Supplementary Fig. 15a, b).

We next examined the leaf cuticle of *ACL1-D*, ACL1KO, and ZH11 plants using transmission electron microscopy (TEM), and revealed that the basic structure of the cuticle membrane was similar among the three lines. However, the cuticle thickness differed markedly, with that of ACL1KO thicker and that of *ACL1-D* thinner, compared with that of ZH11 (Fig. 2h–k).

Because wax content might influence the permeability of the leaf surface, we further examined the water-loss efficiency of the *ACL1-D*, ACL1KO, and ZH11 plants. The fresh weight of the *ACL1-D* plants decreased much more quickly than that of ZH11 plants, whereas that of the ACL1KO plants decreased much more slowly, corresponding with higher and lower water-loss efficiencies, respectively (Fig. 2l). We further detected the chlorophyll leaching rate. Although the ACL1KO plants did not show a significant difference from ZH11, *ACL1-D* plants showed a much higher rate of chlorophyll leaching (Fig. 2m). In conclusion, *ACL1* negatively regulated the wax content on the plant surface, which in turn influenced water permeability.

ACL1 interacts with almost all ROC proteins in rice

Being a small peptide, ACL1 might function through forming complexes with other proteins. Therefore, we searched the potential interacting proteins of ACL1 using the TurboID system[49,50]. We first constructed Turbo-ACL1 and Turbo transgenic plants (Supplementary Fig. 16a). As expected, the Turbo-ACL1 plants showed *ACL1* overexpression (Supplementary Fig. 16b), with the Turbo-ACL1 fusion protein readily detectable (Supplementary Fig. 16c). The Turbo-ACL1 plants showed abaxial leaf-rolling, while the Turbo plants did not (Supplementary Fig. 16d). Thus, the fused Turbo protein did not disturb with the function of ACL1.

We then used the Turbo-ACL1 and Turbo plants for immunoprecipitation assays, followed by protein liquid chromatography-mass spectrometry (LC-MS) assay. After filtering with the proteins identified in ZH11 and Turbo plants, 774 proteins in the Turbo-ACL1 plants were screened as putative interacting proteins for ACL1 (Supplementary Fig. 17a and Supplementary Data 1). Among these proteins, ROC2, ROC5, and ROC7 belonging to the homeodomain leucine zipper IV (HD-Zip IV) transcription factor family, were screened with a high peptide count (Supplementary Fig. 17b and Supplementary Data 1). Given that most ROCs are specific to epidermal or sub-epidermal cells[51], and considering the epidermal expression pattern of *ACL1* (Fig. 1c and Supplementary Fig. 4b), we further verified the interaction between ACL1 and these ROCs. In total, nine genes encode ROC proteins in rice (Supplementary Fig. 18a)[51]. While transcripts of *ROC9* were barely detectable, other *ROC*s showed relatively high expression levels in the leaves (Supplementary Fig. 18b). We cloned the *ROC*s and performed yeast two-hybrid (Y2H) (Supplementary Fig. 19), bimolecular fluorescence complementation (BIFC) (Supplementary Fig. 20), luciferase complementation imaging (LCI) (Fig. 3a), and Co-immunoprecipitation (Co-IP) assays (Fig. 3b). All assays confirmed the interaction between ACL1 and each ROC.

ACL1 competes with the ROC4–ROC4 and ROC5–ROC5 homodimers, and the ROC4–ROC5 heterodimer

Plant HD-Zip family members function via homodimers and heterodimers[52,53]. Therefore, we examined dimer formation by ROC4

https://doi.org/10.1038/s41467-024-52436-w

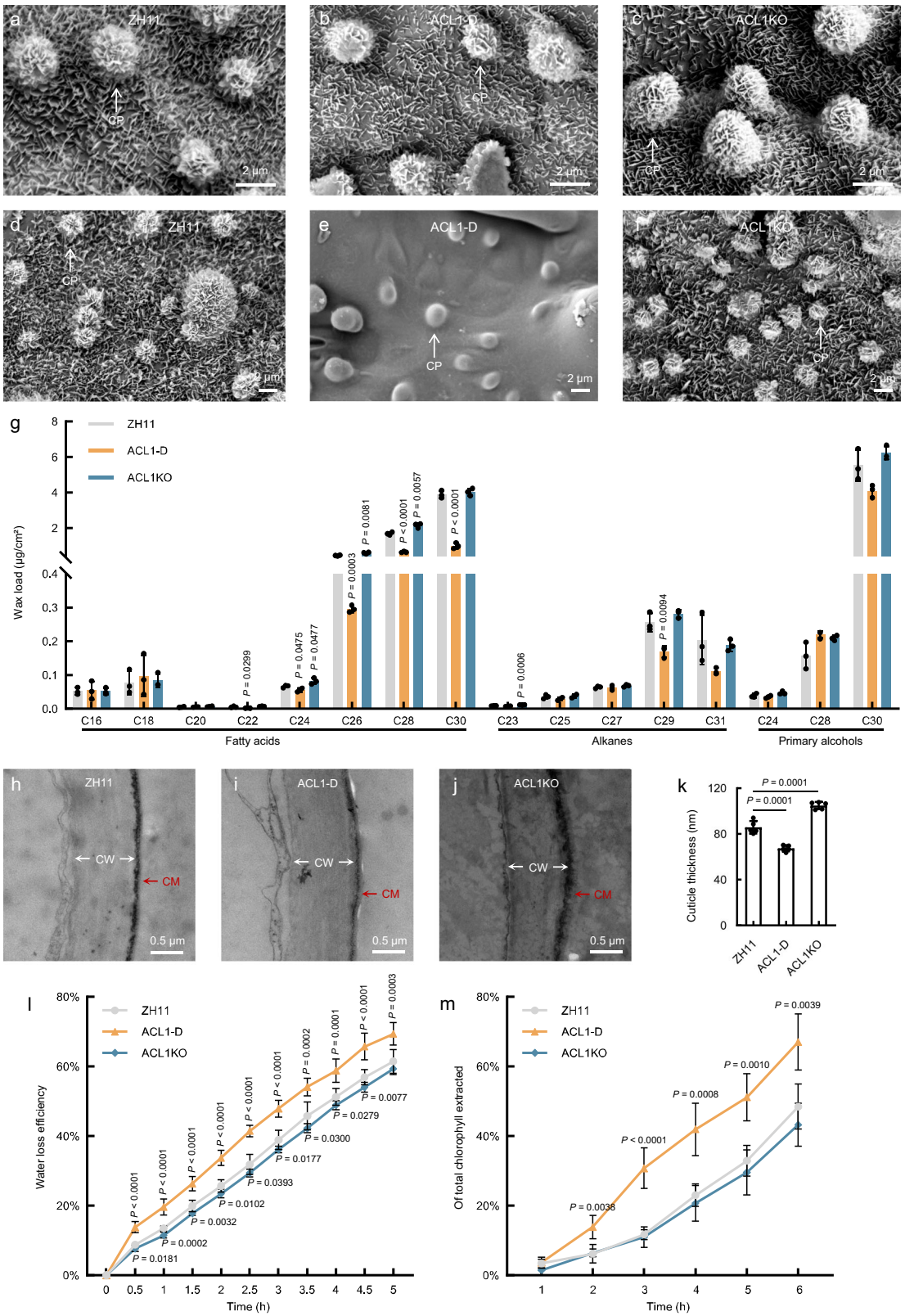

Fig. 2 | Wax status and leaf permeability of *ACL1-D*, ACL1KO, and ZH11 plants. **a**–**c** SEM micrographs of the flag leaf surface of ZH11 (**a**), *ACL1-D* (**b**), and ACL1KO (**c**). **d**–**f** SEM of the leaf sheath surface of ZH11 (**d**), *ACL1-D* (**e**), and ACL1KO (**f**). Bars in (**a**–**f**) are 2 μm. CP, cuticular papillae. **g** Wax content in leaves of the *ACL1-D*, ACL1KO, and ZH11 plants revealed by GC-MS. Data are means ± SD ($n = 3$). **h**–**j** Transmission electron micrographs of the cuticle on the adaxial leaf surface of ZH11, *ACL1-D*, and ACL1KO plants. Bars are 0.5 μm. CW, cell wall. CM, cuticle membrane. **k** Thickness of the leaf cuticle in ZH11, *ACL1-D*, and ACL1KO plants. Data are means ± SD ($n = 5$). **l** Water-loss efficiency of the leaves of *ACL1-D*, ACL1KO, and ZH11 plants. Data are means ± SD ($n = 8$). **m** Chlorophyll leaching rate of the leaves of *ACL1-D*, ACL1KO, and ZH11 plants. Data are means ± SD ($n = 5$). The *P*-values in (**g**) and (**k**–**m**) were determined by a two-tailed unpaired Student's t-test. Source data are provided as a Source Data file.

https://doi.org/10.1038/s41467-024-52436-w

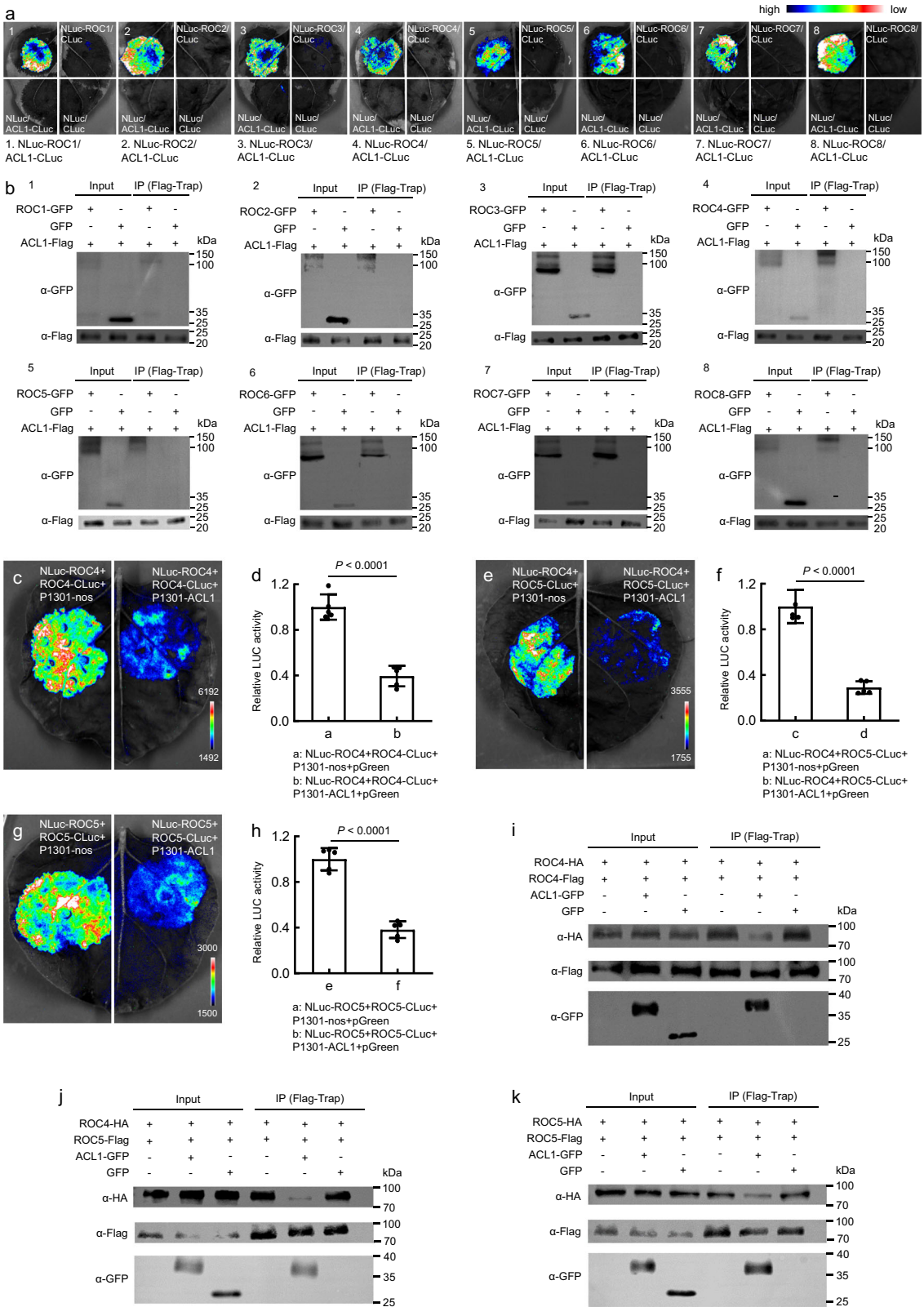

and ROC5. When NLuc-ROC4 was co-expressed with ROC4-CLuc in *Nicotiana benthamiana* leaves, the luciferase (LUC) signal was strong (Fig. 3c and Supplementary Fig. 21a), indicating that ROC4 could form a homodimer. However, when ACL1 was added, the interaction between ROC4-CLuc and NLuc-ROC4 was weaker, as indicated by the decreased LUC signal and relative LUC activity (LUC/REN) (Fig. 3c, d). Similarly, when NLuc-ROC4 was co-expressed with ROC5-CLuc, the LUC signal was strong (Fig. 3e and Supplementary Fig. 21b), indicating that ROC4 could form a heterodimer with ROC5. However, in the presence of ACL1, the LUC signal and the relative LUC activity were decreased (Fig. 3e, f). When NLuc-ROC5 was co-expressed with ROC5-CLuc, the LUC signal was strong (Fig. 3g and Supplementary Fig. 21c).

Fig. 3 | Interaction between ACL1 and ROC1-8 proteins and ACL1 competition with ROC4/ ROC5 in the formation of homo-dimers and hetero-dimers. a LCI assay to detect the interaction between ACL1 and ROC1-8 proteins as indicated, respectively. **b** Co-IP assay to detect the interaction between ACL1 and ROC1-8 proteins as indicated respectively. 1–8, Co-IP of ACL1 and ROC1, ROC2, ROC3, ROC4, ROC5, ROC6, ROC7 and ROC8, respectively. **c** LCI assay indicating competition of ACL1 with ROC4–ROC4 homodimerization. **d** Relative LUC activity (LUC/REN) in (**c**). **e** LCI assay indicating competition of ACL1 with ROC4–ROC5 heterodimerization. **f** Relative LUC activity (LUC/REN) in (**e**). **g** LCI assay indicating competition of ACL1 with ROC5–ROC5 homodimerization. **h** Relative LUC activity (LUC/REN) in (**g**). Data in (**d**), (**f**), and (**h**) are means ± SD ($n = 5$), and the *P*-values were determined by a two-tailed unpaired Student's *t* test. **i**–**k** Co-IP assay showing competition of ACL1 with ROC4–ROC4 homodimerization (**i**), ROC4–ROC5 heterodimerization (**j**) and ROC5–ROC5 homodimerization (**k**). In (**i**), (**j**), and (**k**), the three left lanes showed the protein immunoblots of input controls with anti-HA, anti-GFP, and anti-Flag antibodies. The right three lanes showed the results of Co-IP. The Flag-Trap was used for the co-immunoprecipitation. The experiments in (**b**) and (**i**–**k**) were repeated at least three times with similar results. Source data are provided as a Source Data file.

However, in the presence of ACL1, the LUC signal and the relative LUC activity was decreased (Fig. 3g, h). These assays indicated that ACL1 interfered with the formation of ROC4–ROC4, ROC4–ROC5, and ROC5–ROC5 homodimers and heterodimers.

We further performed a competitive Co-IP assay. Consistently, ROC4-HA was co-immuno-precipitated by ROC4-Flag with Flag-Trap (Fig. 3i). When ACL1-GFP, but not GFP alone, was co-expressed with ROC4-HA and ROC4-Flag, the amount of ROC4-HA co-immuno-precipitated by ROC4-Flag was decreased markedly (Fig. 3i), indicating that homodimerization of ROC4 was decreased by ACL1. Similarly, both heterodimerization of ROC4 and ROC5 (Fig. 3j), and homodimerization of ROC5 was disrupted by ACL1 (Fig. 3k).

ROC4 positively regulates drought tolerance, BPH resistance, and wax content

Several *ROC*s have been reported to regulate leaf-rolling in rice, such as *ROC5*[35] and *ROC8*[38,52]. Specifically, the *roc5* and *roc8* mutants show increased number and size of BCs similar to *ACL1-D* plants. *ROC4* has been reported to mediate drought tolerance through the regulation of wax synthesis[21]. Given that ACL1 interacted with ROCs, we analyzed the genetic function of ROC4 in drought tolerance and BPH resistance.

We constructed the ROC4KO and ROC4OE plants and selected two lines each for further functional analysis. In both ROC4OE lines, *ROC4* was up-regulated (Supplementary Fig. 22a), and in both ROC4KO lines, it was successfully edited (Supplementary Fig. 22b). SEM examination revealed that, in the ROC4KO plants, wax was more sparsely distributed on the leaves, whereas in the ROC4OE plants, wax was much more densely distributed (Fig. 4a). A GC-MS analysis verified that the wax content was lower in the ROC4KO-1 leaves, but higher in the ROC4OE-24 leaves (Fig. 4b). We further conducted drought tolerance and BPH resistance assays. When treated with 20% PEG6000, the survival of ROC4KO plants was lower than that of ZH11 (Fig. 4c, d), whereas the ROC4OE plants showed a higher survival rate than ZH11 (Fig. 4e, f). Furthermore, in response to water cut-off, the drought sensitivity of both ROC4KO lines and the drought tolerance of both ROC4OE lines were verified (Supplementary Fig. 23). In both individual tests and small population tests for BPH resistance detection, both ROC4KO lines died earlier than the WT (Fig. 4g, h, j), with lower survival rates than that of WT (Fig. 4i, k). In contrast, both ROC4OE lines died later than the WT (Fig. 4l, m, o), with higher survival rates (Fig. 4n, p). Therefore, *ROC4* positively regulated drought tolerance, BPH resistance, and wax content concurrently in rice.

ROC5 is required for drought tolerance and BPH resistance

We constructed ROC5KO plants (Supplementary Fig. 24a), which developed abaxially rolled leaves (Supplementary Fig. 24b) similar to the *roc5* mutant[35]. In direct water cut-off, the ROC5KO plants were more highly sensitive to drought than the WT plants (Fig. 5a), with a lower survival rate (Fig. 5b). When treated with 20% PEG6000, similar results were obtained (Fig. 5c, d). Meanwhile, in both kinds of BPH resistance tests, the ROC5KO plants died earlier than ZH11 plants (Fig. 5e, f) and had a lower survival rate (Fig. 5g). Thus, ROC5KO plants were sensitive to drought and vulnerable to BPH infestation. Similar results were obtained using the *roc5* mutant and WT NIP. The *roc5* mutant was susceptible to BPH whether in individual tests or small population tests (Supplementary Fig. 25a, b), with a lower survival rate (Supplementary Fig. 25c). In direct water cut-off (Supplementary Fig. 25d, e) and 20% PEG6000 treatment (Supplementary Fig. 25f, g), the *roc5* mutant was more sensitive to drought than NIP. Thus, the *ROC5* gene was required for both drought tolerance and BPH resistance.

Overexpression of *ROC4* and *ROC5* in *ACL1-D* recovers the drought-sensitive, BPH-susceptible, wax content, and leaf-rolling phenotypes

We investigated the genetic interaction of *ACL1* with *ROC4* and *ROC5*. First, we overexpressed *ROC4* in *ACL1-D* and generated 4OE/*ACL1-D* plants. Expression of both *ACL1* and *ROC4* in 4OE/*ACL1-D* plants was higher than that in ZH11 (Supplementary Fig. 26a). Next, in direct water cut-off assay, the drought sensitivity of the *ACL1-D* plants was recovered in the 4OE/*ACL1-D* plants (Fig. 5h), and the survival rate of 4OE/*ACL1-D* plants was similar to that of ZH11, which for both lines was much higher than that of *ACL1-D* (Fig. 5i). In BPH resistance assays, the *ACL1-D* plants died earlier than ZH11 and 4OE/*ACL1-D* plants in both individual test (Fig. 5j) and small population test (Fig. 5k), and the survival rates of ZH11 and 4OE/*ACL1-D* plants were similar, which for both lines was much higher than that of *ACL1-D* (Fig. 5l). Therefore, overexpression of *ROC4* recovered the drought sensitivity and BPH susceptibility of *ACL1-D* plants. We conducted an SEM examination to determine if this recovery was associated with wax content. The wax on the leaf surface of ZH11 and 4OE/*ACL1-D* plants was similar, both much denser than that on the *ACL1-D* leaf surface (Fig. 5r). Furthermore, GC-MS analysis revealed that the wax content of 4OE/*ACL1-D* plants showed no difference to that of ZH11 (Supplementary Fig. 27a). Therefore, the reduced wax content of *ACL1-D* plants was recovered by *ROC4* overexpression.

Meanwhile, we overexpressed *ROC5* in *ACL1-D* and generated 5OE/*ACL1-D* plants. Expression of both *ACL1* and *ROC5* in the 5OE/*ACL1-D* plants was higher than that in ZH11 (Supplementary Fig. 26b). In direct water cut-off assay, the drought sensitivity of the *ACL1-D* plants was recovered in the 5OE/*ACL1-D* plants (Fig. 5m), and the survival rate of 5OE/*ACL1-D* plants was similar to that of ZH11, which for both was much higher than that of *ACL1-D* (Fig. 5n). In BPH resistance assays, the *ACL1-D* plants died earlier than the ZH11 and 5OE/*ACL1-D* plants in both individual test and small population test (Fig. 5o, p), and the survival rates of ZH11 and 5OE/*ACL1-D* plants were similar, which for both was much higher than that of *ACL1-D* (Fig. 5q). Therefore, overexpression of *ROC5* recovered the drought sensitivity and BPH susceptibility of *ACL1-D* plants. A SEM analysis revealed that the wax on the leaf surface of ZH11 and 5OE/*ACL1-D* plants was similar, both much denser than that on the *ACL1-D* leaf surface (Fig. 5r). Furthermore, GC-MS analysis revealed that the wax content in 5OE/*ACL1-D* plants showed no difference to that in ZH11 (Supplementary Fig. 27b). Therefore, the reduced wax content in *ACL1-D* plants was recovered by *ROC5* overexpression. Interestingly, in neither the ROC5OE nor the ROC5KO plants, the wax content was different from than in ZH11

https://doi.org/10.1038/s41467-024-52436-w

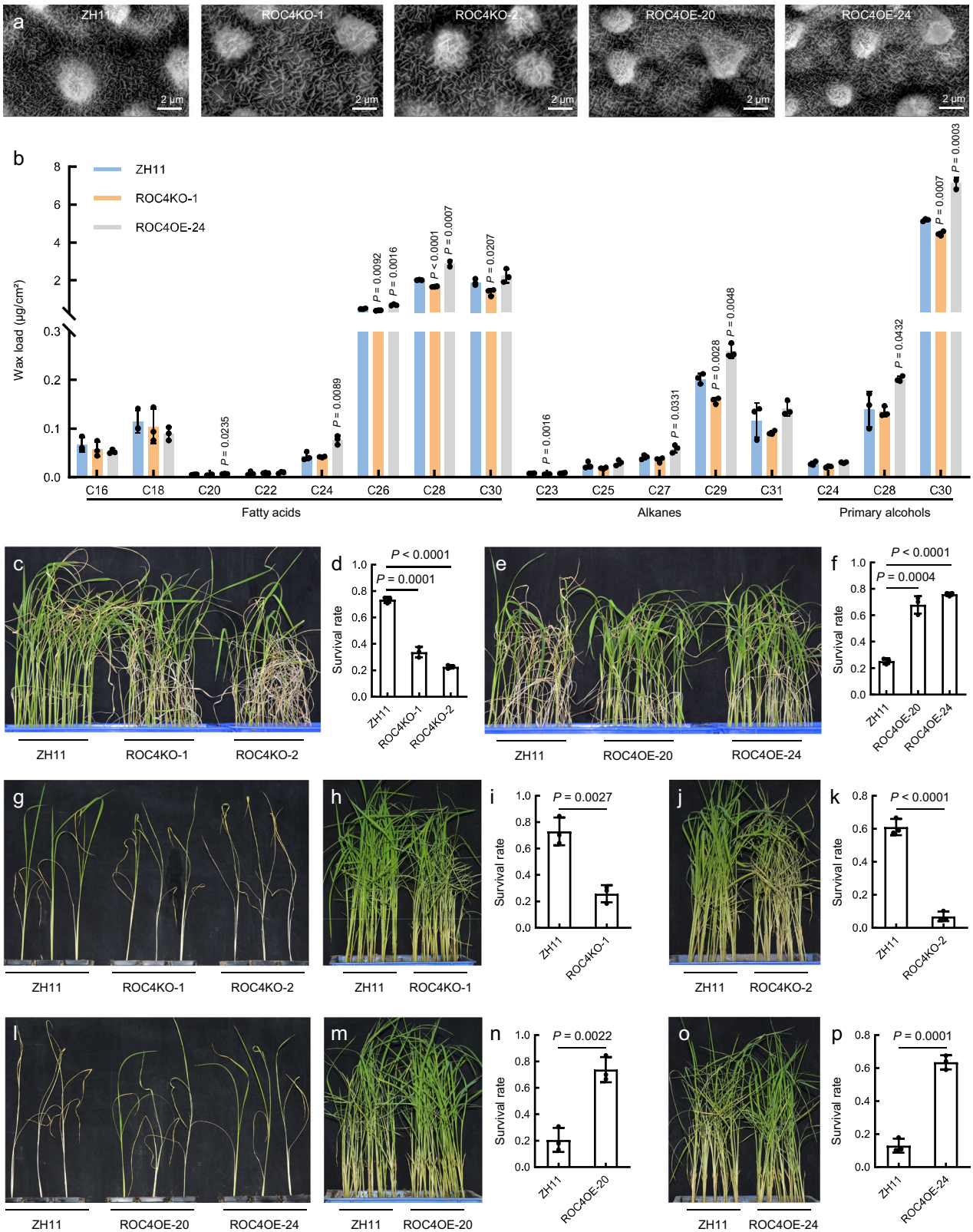

Fig. 4 | Genetic function of *ROC4* in rice. a SEM micrographs of the leaf surface of ROC4KO-1, ROC4KO-2, ROC4OE-20, ROC4OE-24, and ZH11 plants to reveal the wax status. Bars are 2 μm. **b** GC-MS assay of the wax content in the leaves of ROC4KO-1, ROC4OE-24, and ZH11 plants. **c** Phenotype of ROC4KO-1, ROC4KO-2, and ZH11 plants after 20% PEG6000 treatment. Uniformly grown plants were treated for 9 days before re-watering. **d** Survival of the plants in (**c**). **e** Phenotype of ROC4OE-20, ROC4OE-24, and ZH11 plants after 20% PEG6000 treatment. Uniformly grown plants were treated for 11 days before re-watering. **f** Survival of the plants in (**e**). **g**, **h**, **j** Phenotype of ROC4KO-1, ROC4KO-2, and ZH11 plants after BPH infestation in an individual test (**g**) and small population test (**h**, **j**). **i**, **k** Survival of the plants in (**h**) and (**j**). **l**, **m**, **o** Phenotype of ROC4OE-20, ROC4OE-24, and ZH11 plants after BPH infestation in an individual test (**l**) and small population test (**m**, **o**). **n**, **p** Survival of the plants in (**m**) and (**o**). Data are means ± SD ($n = 3$). Data in (**b**), (**d**), (**f**), (**i**), (**k**), (**n**), and (**p**) are means ± SD ($n = 3$), and the *P*-values were determined by two-tailed unpaired Student's *t* test. Source data are provided as a Source Data file.

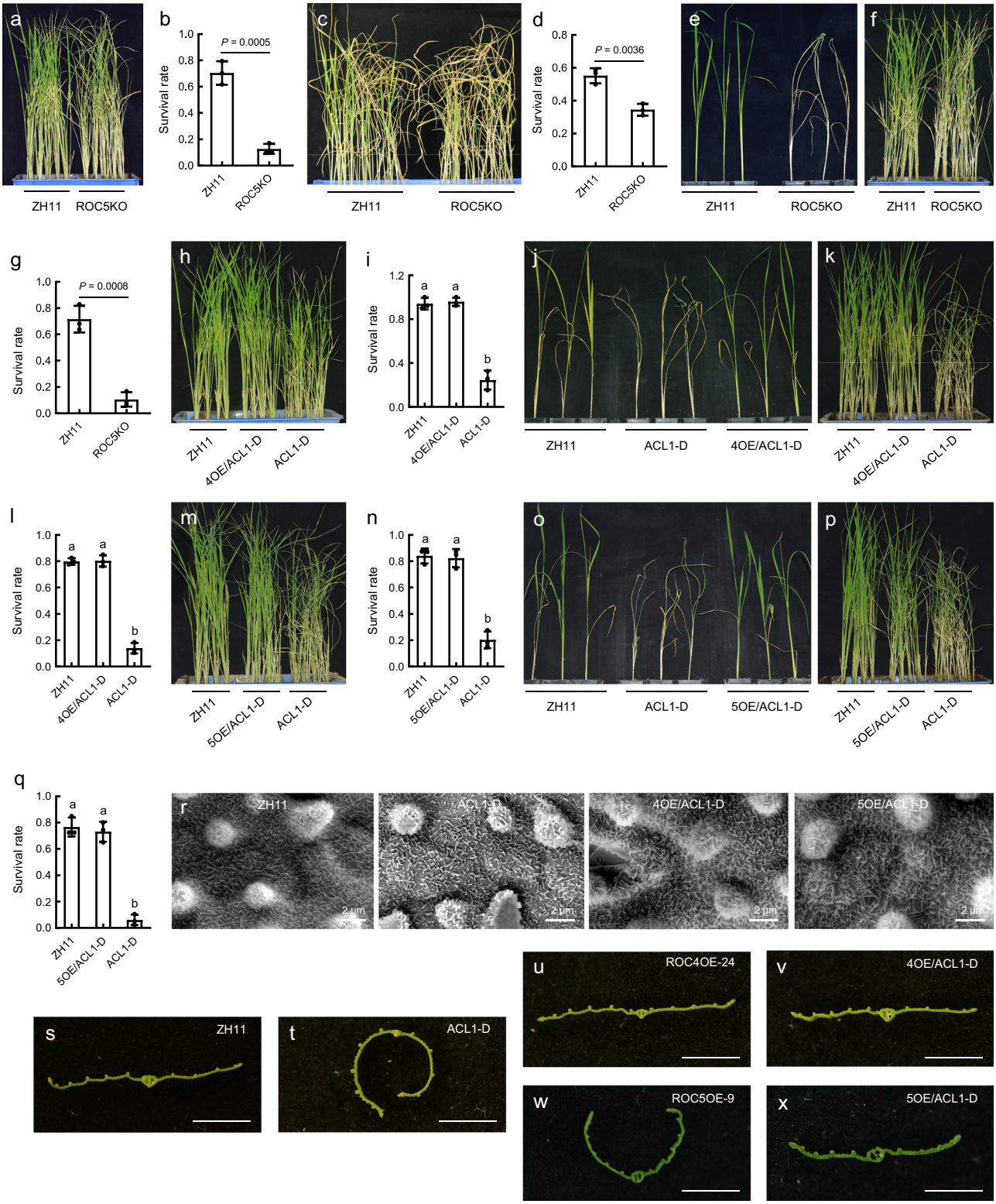

(Supplementary Fig. 28). Although in ROC5OE plants, *ROC5* was up-regulated (Supplementary Fig. 24c) and the leaf was adaxially rolled, while in ROC5KO plants the leaf was abaxially rolled (Supplementary Fig. 24b).

We examined the leaf-rolling phenotypes of the 4OE/*ACL1-D* and 5OE/*ACL1-D* plants. Although the ROC4OE leaf did not roll adaxially (Fig. 5s, u), the 4OE/*ACL1-D* leaf was flat as in ZH11, recovering the abaxial leaf-rolling phenotype of *ACL1-D* (Fig. 5s, t, v). The 5OE/*ACL1-D* leaf was flat (Fig. 5s, x), intermediate between the adaxially rolled ROC5OE leaf (Fig. 5w) and the abaxially rolled *ACL1-D* leaf (Fig. 5t). Thus, the leaf-rolling phenotype of *ACL1-D* plants was recovered by respective overexpression of *ROC4* and *ROC5*.

To sum up, respective overexpression of *ROC4* and *ROC5* in *ACL1-D* recovered the drought-sensitive, BPH-susceptible, low wax content, and the leaf-rolling phenotypes simultaneously.

Fig. 5 | Characterization of drought tolerance and BPH infestation in ROC5KO plants, and recovery of *ACL1-D* plants from *ROC4* and *ROC5* overexpression. **a** Phenotype of ROC5KO and ZH11 plants after direct water cut-off. Uniformly grown plants were treated for 6 days before re-watering. **b** Survival of the plants in (**a**). **c** Phenotype of ROC5KO and ZH11 plants after 20% PEG6000 treatment. Uniformly grown plants were treated for 11 days before re-watering. **d** Survival of the plants in (**c**). **e**, **f** Phenotype of ROC5KO and ZH11 plants after BPH infestation in an individual test (**e**) and small population test (**f**). **g** Survival of the plants in (**f**). **h** Phenotype of ZH11, *ACL1-D*, and 4OE/ACL1-D plants after direct water cut-off. Uniformly grown plants were treated for 6 days before re-watering. **i** Survival of the plants in (**h**). **j**, **k** Phenotype of ZH11, *ACL1-D*, and 4OE/ACL1-D plants after BPH infestation in an individual test (**j**) and small population test (**k**). **l** Survival of the plants in (**k**). **m** Phenotype of ZH11, *ACL1-D*, and 5OE/ACL1-D plants after direct water cut-off. Uniformly grown plants were treated for 6 days before re-watering. **n** Survival of the plants in (**m**). **o**, **p** Phenotype of ZH11, *ACL1-D*, and 5OE/ACL1-D plants after BPH infestation in an individual test (**o**) and small population test (**p**). **q** Survival of the plants in (**p**). **r** SEM micrographs of the leaf surface of ZH11, *ACL1-D*, 4OE/ACL1-D, and 5OE/ACL1-D plants. Bars are 2 μm. **s**–**x** Transverse sections of leaves of ZH11, *ACL1-D*, ROC4OE-24, 4OE/ACL1-D, ROC5OE-9, and 5OE/ACL1-D leaves. The bars are 0.5 cm. Data in (**b**), (**d**), (**g**), (**i**), (**l**), (**n**), and (**q**) are means ± SD ($n = 3$). The *P*-values in (**b**), (**d**), and (**g**) were determined by a two-tailed unpaired Student's t-test. Different letters in (**i**), (**l**), (**n**), and (**q**) indicated significant differences determined by one-way ANOVA with two-sided Tukey's HSD test ($P < 0.01$). *P*-values are shown in the Source Data file.

ACL1 might suppress the function of ROCs through forming a repressor complex with TOPLESS

Given that ACL1 inhibited the function of the ROCs, we evaluated whether ACL1 could recruit the transcriptional corepressor TOPLESS-related proteins (TPRs), the typical family of corepressors that are critical for various plant life processes[54], to form repressor complexes. First, using the TurboID system, the three TPRs in rice, TPR1, TPR2, and TPR3 were filtered as neighboring proteins of ACL1 (Supplementary Fig. 29a and Supplementary Data 1). An EAR motif was detected in the ACL1 protein, which typically mediates the interaction with TPRs, indicating possible interaction with TPRs (Supplementary Fig. 29b). In a Y2H assay, ACL1 could interact with the N-terminals of all three TPR proteins (Fig. 6a and Supplementary Fig. 29c), but not the full-length TPRs (Supplementary Fig. 29d). A LCI assay revealed that only the combination of TPR3 and ACL1 showed strong fluorescence signal when the full-length TPRs was used (Supplementary Fig. 29e); when the N-terminals were used, all three TPRs could interact with ACL1 (Fig. 6b).

It is reported that ROC4 regulates cuticular wax biosynthesis through regulating the BODYGUARD (*BDG*) gene[21]. We detected the expression of the *BDG* gene in the ZH11, ROC4KO, ROC4OE, *ACL1-D*, ACL1KO, and 4OE/ACL1-D plants. Consistently, it was down-regulated in the *ACL1-D* and ROC4KO plants but promoted in the ROC4OE and ACL1KO plants; in the 4OE/ACL1-D plants, *BDG* expression was distinctly promoted, but the expression remained lower than that in the ROC4OE plants (Fig. 6c).

The downstream gene of *ROC5*, the *Protodermal Factor Like* (*PFL*), negatively regulates BC development, and the corresponding RNAi plants show abaxially rolled leaves[35]. We analyzed the expression of *PFL* in ZH11, ROC5KO, ROC5OE, *ACL1-D*, ACL1KO, and 5OE/ACL1-D plants. Consistently, *PFL* was down-regulated in the *ACL1-D* and ROC5KO plants but promoted in the ROC5OE and ACL1KO plants; in the 5OE/ACL1-D plants, *PFL* expression was distinctly promoted, but its expression remained lower than that in ROC5OE plants (Fig. 6d).

In summary, ACL1 repressed the function of ROC4 and ROC5, which positively regulated the *BDG* gene in wax biosynthesis and the *PFL* gene in BC development, respectively.

ACL1–ROC4/5 complexes synergistically regulate drought tolerance and BPH resistance

We analyzed if ROC4/5 could interact with TPRs. In a Y2H assay, neither ROC4 nor ROC5 interacted with the full-length or the N-terminals of the three TPRs (Supplementary Fig. 30). In an LCI assay, the combination of ROC5 and the N-terminals of TPR1 and TPR2 showed fluorescence signals, whereas no signals were detected in the combination of ROC4 with TPRs (Supplementary Fig. 31). Thus, ROC5 might interact with TPR1/2.

Taken together, the present results revealed the putative mechanism by which ACL1–ROC4/5 complexes synergistically regulated drought tolerance and BPH resistance. When there is less ACL1, more ROCs are released from the ACL1–ROCs complexes to form homodimers or heterodimers to regulate downstream genes. Specifically, ROC4 regulates wax synthesis genes to promote wax accumulation on the leaf and sheath surface, and ROC5 regulates genes to inhibit the over-development of BCs on the adaxial epidermis, thus promoting drought tolerance and BPH resistance (Fig. 6e, left panel). Excessive ACL1 competitively binds with ROC4 and ROC5 to obstruct homodimer or heterodimer formation, and recruits TOPLESS to inhibit the downstream transcription of wax biosynthetic genes and BC-related genes, thus resulting in less wax, and increase in the number and size of BCs, which promotes susceptibility to both drought and BPH (Fig. 6e, right panel).

Discussion

Trichomes are specialized epidermal cells that deter insects. Similarly, BCs are specialized epidermal cells specific to the Poaceae that function in stress response, but the underlying mechanism remains unclear. In maize, BCs have a specialized water-permeable cuticle and shrink differentially during leaf dehydration[55]. Here, we showed that in rice, upon drought exposure and BPH infestation, the BCs shrank (Fig. 1a) and adaxial leaf-rolling occurred (Supplementary Fig. 1). The *ACL1-D* mutant, with an increase in number and size of BCs, was more sensitive to drought (Fig. 1d and Supplementary Fig. 8) and BPH infestation (Fig. 1e–g), and had a decreased cuticular wax content, which might promote water permeation (Fig. 2). Furthermore, in the ACL1KO and ACLDKO plants, the wax contents were increased (Fig. 2c, f, g and Supplementary Fig. 15), and accordingly, the ACL1KO and ACLDKO plants were more strongly resistant to BPH (Fig. 1i–p) and drought tolerant (Fig. 1d and Supplementary Fig. 8, 9). Consistently, the ACL1-interacting ROC5 functions to inhibit BC development, and in the ROC5KO plants, the BC number and size were increased, resulting in abaxial leaf-rolling (Supplementary Fig. 24b), similar to that of *ACL1-D*. In addition, the ROC5KO plants were drought-sensitive (Fig. 5a–d) and BPH-susceptible (Fig. 5e–g). Therefore, the BCs are responsive in stresses-induced leaf-rolling in rice, to which the parenchymatous cell characteristics, together with the wax covering might contribute.

The cuticle forms a hydrophobic waxy layer that covers plant organs and provides physical protection from biotic and abiotic stresses. Accumulation of cuticular waxes contributes to drought tolerance[56], and some transcription factors modulate drought tolerance by regulating the wax content[19,57]. The wax content was greatly decreased in *ACL1-D* plants (Fig. 2b, e, g), but was increased in ACL1KO plants (Fig. 2c, f, g), indicating possible involvement of wax in ACL1-mediated drought tolerance and BPH resistance. Consistently, the ACL1-interacting ROC4 positively regulated the wax content, which was increased in ROC4OE but decreased in ROC4KO plants (Fig. 4a, b). As a result, ROC4OE plants were drought tolerant (Fig. 4e, f and Supplementary Fig. 23e–h) and BPH resistant (Fig. 4l–p), whereas ROC4KO plants were drought sensitive (Fig. 4c, d and Supplementary Fig. 23a–d) and BPH susceptible (Fig. 4g–k). Therefore, ACL1–ROC4 might modulate BPH resistance and drought tolerance by regulating the wax content. ROC4 directly regulates wax biosynthesis genes[21], and ACL1 modulated ROC4 through direct interaction at the protein level (Fig. 3a, b), which disrupted the formation of ROC4 homodimers

https://doi.org/10.1038/s41467-024-52436-w

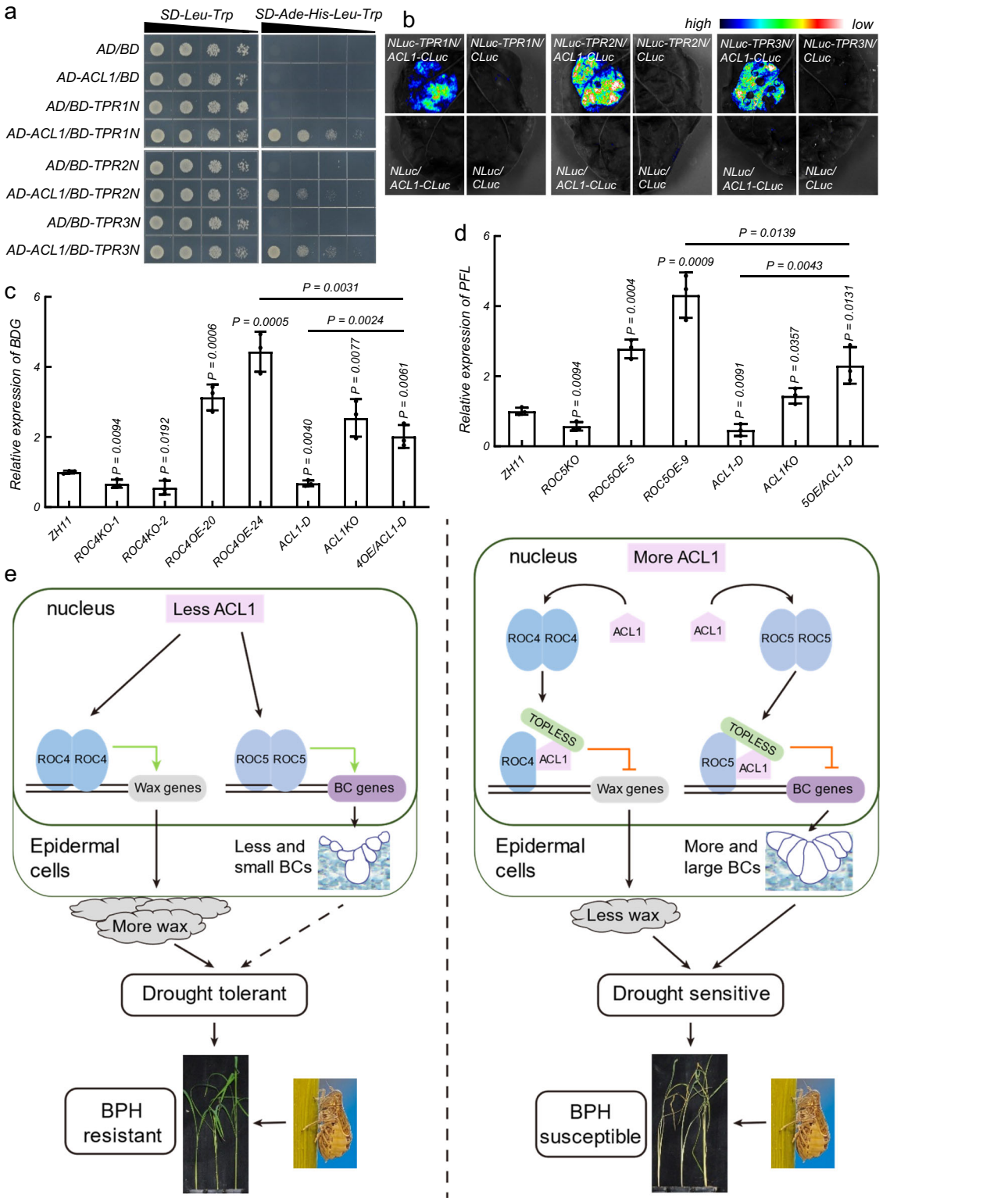

Fig. 6 | ACL1 recruits TOPLESS to repress ROCs in the regulation of wax content and bulliform cells to synergistically modulate drought tolerance and BPH resistance. a Y2H of ACL1 interacting with the N-terminals of three TPRs. **b** LCI assay of ACL1 interacting with the N-terminals of three TPRs. **c** Expression of *BDG* in different genotypes. **d** Expression of *PFL* in different genotypes. Data in (**c**) and (**d**) are means ± SD ($n = 5$), and the *P* values were determined by a two-tailed unpaired Student's t-test. Source data are provided as a Source Data file. **e** Model of ACL1–ROC4/5 complexes synergistically regulating drought tolerance and BPH resistance. When there are fewer ACL1 proteins, more ROC proteins are released to form homodimers or heterodimers. ROC4 regulates wax synthesis genes to promote wax synthesis, and ROC5 regulates BC-related genes to inhibit the over-development of BC, thus promoting drought tolerance and increasing BPH resistance of the plants (left panel). Excessive ACL1 proteins could competitively bind with ROC4 and ROC5 to obstruct homodimer or heterodimer formation and recruit TOPLESS to form a complex to inhibit the downstream transcription of wax biosynthesis genes and BC-related genes, thus resulting in decreased wax content and an increase in the number and size of BCs, which promotes susceptibility to both drought and BPH (right panel).

(Fig. 3c, d, i), and/or heterodimers with other ROCs, such as ROC5 (Fig. 3e, f, j).

The *ACL1* gene showed an epidermal expression pattern (Fig. 1c). In accordance, over-expression of *ACL1* resulted in an increase in number and size of BCs, which resulted in abaxial leaf-rolling[30] (Supplementary Fig. 6c). The homologous genes of *ACL1* in *Arabidopsis*, *GIR1* and *GIR2*, regulate root hair formation and also show an epidermal expression pattern[58]. Overexpression of *GIR1* in rice resulted in abaxially rolled leaves (Supplementary Fig. 6j), and enhanced drought sensitivity (Supplementary Fig. 10) and BPH susceptibility (Supplementary Fig. 12a–d), indicating the functional conservation of *ACL1* in *Arabidopsis* and rice not only in development but also in response to biotic and abiotic stresses. In *Arabidopsis*, GIR1 and GIR2 interact with GLABRA2[58], a typical HD-Zip IV protein that suppresses root hair differentiation as well as initiates leaf trichome development[59,60]. Here, we showed that ACL1 interacted with HD-Zip IV family ROC proteins, which show a typical epidermal expression pattern and functioning[51]. The ACL1–ROC interaction is also conserved in tomato, with the Woolly (HD-Zip IV) and SlCycB2 (homologous to ACL1) pair regulating trichrome formation[61]. Furthermore, NtCycB2 in *Nicotiana tabacum* negatively regulates trichome development and aphid resistance[62]. Thus, the epidermal ACL1–ROC complex might be conserved among different plant species. The HD-Zip IV proteins drive the differentiation of epidermal cells[63], ACL1 might be a conserved co-factor of HD-Zip IV. The extent to which the ACL1–ROC complex functions in the plant kingdom deserves further research.

The insect-feeding behavior (piercing–sucking versus chewing) is a decisive determinant of the plant's defense response[64]. The interaction between rice and BPH is typical for piercing-sucking insects. Although increasing evidence indicates the similarity between the perception mechanism and the following response signal transduction for resistance to BPH and microbial pathogens[12,13], a more specific genetic and molecular mechanism based on the particular feeding behavior might be neglected. The response to piercing-sucking insects is usually not associated with a strong wound response, as is the case for chewing insects, but might be strongly associated with the drought response because the sap is directly sucked out from the phloem during feeding. In accordance with this hypothesis, we revealed that the ACL1–ROC5 and ACL1–ROC4 pathways synergistically regulate drought tolerance and BPH resistance through regulation of BC development and cuticular wax content, respectively (Fig. 6e). Strict coordination might exist between the ACL1–ROC4 and ACL1–ROC5 pairs, given that ROC4 and ROC5 could interact and that ACL1 could compete with the ROC4–ROC5 heterodimer (Fig. 3e, f, j). Whether the mechanism of the epidermal ACL–ROCs complex is also applicable to other types of interaction between piercing-sucking insects and host plants requires further study. If applicable, the wax content might be a conserved downstream factor mediating the resistance to insects. However, the Poaceae-specific BCs might be modified into other specialized epidermal cell types in other plant species, such as trichomes, that could deter insects.

All together, we discovered a kind of ACL1–ROCs complexes in rice that could synergistically regulate drought tolerance and BPH resistance through modulating two kinds of typical physical barriers in the plant surface, BCs and cuticular wax content (Fig. 6e). With increased wax content and/or shrunk BCs, the rice plants are more tolerant to drought and resistant to BPH (Fig. 6e, left panel). On the contrary, with increased BCs and/or decreased wax content, rice plants are more susceptible to BPH and more vulnerable to drought (Fig. 6e, right panel).

Methods

Plant species and growth conditions

The wild-type (WT) rice plants were varieties ZH11 (*Oryza sativa* L. subsp. *japonica* cv. Zhonghua No.11, ZH11), NIP (Japonica. cv. *Nip*pobare, NIP), RHT (Rathu Heenati) and TN1 (*indica* cv. Taichung Native 1, TN1). ZH11 and NIP were mainly used as hosts of genetic transformation or natural WT of mutants. RHT was a well-known BPH-resistant variety, and TN1 was used to cultivate BPH. All rice plants were cultivated under field conditions in two experimental stations in Shanghai (30°N, 121°E) and Lingshui (Hainan Province, 18°N, 110°E), China. Rice seedlings were cultured in the phytotron at CAS Center for Excellence in Molecular Plant Sciences, with 30/24 ± 1 °C day/night temperature, 50All Together, we discovered a kind of ACL1–ROCs complexes in rice that could synergistically regulate drought tolerance and BPH resistance through modulating two kinds of typical physical barriers in the plant surface, BCs and cuticular wax content (Fig. 6e).70% relative humidity and a light/dark period of 14 h/10 h.

Plasmid construction and plant transformation

For overexpression of *AtACL1*, *ROC4*, and *ROC5*, full-length cDNA of respective genes were amplified and cloned into p1301-35S-Nos vector through digestion by *Xba*I and *Kpn*I.

For overexpression of *ROC4* and *ROC5* in the *ACL1-D* background, full-length cDNAs were respectively amplified and cloned into the pCAMBIA2301 vector through digestion by *Xba*I and *Kpn*I.

For the construction of pACL1:GUS, the 1.9 kb fragment upstream of the ATG start code of *ACL1* was amplified and cloned into the *Pst*I and *Xba*I sites of the p1300-GUS-Nos plasmid by homologous recombination using the Vazyme ClonExpress® Ultra One Step Cloning Kit.

For the construction of knock-out plants, guider DNA was respectively synthesized and cloned in the pOs-sgRNA vector and then transferred to the pH-Ubi-cas9-7 vector through LR reaction. Primers and gDNAs used were listed in Supplementary Data 2.

For fusion with the Turbo, the *ACL1* sequences were independently amplified and cloned into pCRTM8/GW/TOPO® and then transferred into Gateway-compatible 35S-YFP-miniTurbo vectors by LR reaction[65].

Plasmids were transformed into ZH11 or *ACL1-D* mutants through *Agrobacterium*-mediated genetic transformation in Biorun Biosciences Company.

Calculation of water-loss efficiency

The water-loss efficiency assay was performed as follows. Four-week-old rice seedlings were cut from the base and weighed with a microbalance at 0, 0.5, 1, 1.5, 2, 2.5, 3, 3.5, 4, 4.5, and 5 h. The water-loss efficiency was indicated as follows, (1-the fresh weight at each time point / the initial fresh weight) × 100%. Eight replicates were set in each group.

Chlorophyll leaching assay

Chlorophyll leaching assay was performed as follows. 2 cm segments were removed from the middle part of the second leaf of a 4-week-old seedling, and immediately soaked in 2 ml 80% ethanol, and put in the dark. At 1, 2, 3, 4, 5, 6, and 24 h time points, the absorption spectra at 647 and 664 nm wavelengths were measured by Thermo NANODROP ONE in the order of removal, and the chlorophyll content was equal to 7.93*A664 + 19.53*A647. The chlorophyll leaching rate was calculated as follows, (the chlorophyll content of the samples at each time point/ the chlorophyll content of the samples at 24 h) × 100%. Five replicates were carried out.

TurboID-mediated proximity labeling proteomics

Biotin treatment and protein extraction. Five seedlings of Turbo-ACL1, Turbo, and ZH11, each 7-day-old, were chosen to generate each individual sample. One biological replicate was performed and analyzed via MS. Seedlings were immersed in 50 μM biotin solution for 3 h, and quickly frozen in liquid nitrogen after rinse with ice water. Samples were ground, and added pre-cooled Extraction buffer (50 mM Tris-HCL (pH 7.5), 150 mM NaCl, 0.5% (w/v) sodium deoxycholate,

0.1% (w/v) SDS, 1 mM EDTA, 1 mM DTT, 1 mM PMSF, 10 μg/mL leupeptin and 1× protease inhibitor cocktail), and centrifuged at 10000 × *g*, 15 min, 4 °C to collect the supernatant. Repeat the centrifuge and collection process once.

Protein affinity purification. Biotin was removed from the supernatant using Zeba™ Spin Desalting Columns (Thermo Fisher Scientific). To enrich biotinylated proteins, 30 μl Streptavidin Magnetic Beads (MedChem Express) were added into 2 ml centrifugation tubes, and washed twice with the pre-cooled extraction buffer, then the desalted protein extracts were added and incubated overnight on a 4 °C spinner. Then the magnetic beads were cleaned after magnetic separation according to Mair et al.[49]. Specifically, used cold extraction buffer, cold 1 M KCl, cold 100 mM Na_2CO_3, 2 M Urea in 10 mM Tris pH 8 at room temperature once each, and cold extraction buffer without complete and PMSF twice to clean the magnetic beads. Then 5% magnetic beads were taken for detection by Streptavidin-HRP (Abcam).

Digestion of the beads. The magnetic beads were cleaned with 50 mM ammonium bicarbonate water 3 times. After magnetic separation, 200 μl 10 mM TCEP and 50 mM CAA prepared with 50 mM ammonium bicarbonate were added and incubated at 37 °C for 30 min to redox and alkylate the disulfide bonds. Then digested with trypsin (Promega) at 37 °C overnight after rinse with 50 mM ammonium bicarbonate. The digests were desalted using PIERCE C18 SPIN COLUMNS (Thermo Fisher) and then ran liquid chromatography mass spectrometry (LC-MS) detection.

LC-MS

Experiments were performed on a timsTOF Pro2 mass spectrometer that was coupled to a nano Elute liquid chromatography system (Bruker Daltonics). Samples were reconstituted in 0.1% FA and 200 ng peptide was separated by reversed-phase analytical column (25 cm × 75 μm i.d., Ionopticks) with 60 min gradient (buffer A: 0.1% FA; buffer B: 0.1% FA in ACN) at 2% buffer B followed by a stepwise increase to 22% in 45 min, 37% in 5 min, 80% in 5 min and stayed there for 5 min. The column flow was maintained at 300 nL/min with a column temperature of 50 °C. The timsTOF Pro2 was operated in ddaPASEF mode with the following settings: Capillary Voltage 1500, Dry Gas 3 L/min, Dry Temp 180 °C. During PASEF MS/MS scanning, the collision was ramped linearly as a function of the mobility from 59 eV at 1/K0 = 1.6 V·s/cm2 to 20 eV at 1/K0 = 0.6 V·s/cm2.

Sequence database searching and data analysis

The MS data were analyzed using Paser ver2023 software and searched against the Rice_UP000059680_39947. An initial search was set at a precursor mass window of 10 ppm, followed by an enzymatic cleavage rule of Trypsin and allowed maximal two missed cleavage sites and a mass tolerance of 0.02 Da for fragment ions. Carbamido methylation (C) 57.02 was defined as fixed modification, while protein Oxidiation (M) 15.99 was defined as variable modifications for database searching. The cutoff of the global false discovery rate (FDR) for peptide and protein identification was set to 0.01. The Decoy database was created through a mutated strategy akin to random shuffling of amino acid sequences (ranging from a minimum of 2 amino acids to up to half of the peptide's total length). Spectronaut conducted automatic calibration and data normalization utilizing a local normalization method, and the average peak area of the initial 3 peptides with less than 1.0% false discovery rate (FDR) was employed for protein group quantification.

Phylogenetic analysis

The protein sequence of all the genes was downloaded from the National Center for Biotechnology Information databases (https://www.ncbi.nlm.nih.gov). Phylogenetic trees were generated using predicted full-length amino acid sequences by the maximum-likelihood method in MEGA7.0 with bootstrap mode and 500 replications.

Western blot

Western blot was performed according to the procedures described previously[50].

BPH resistance detection and measurements

The BPH population was originally obtained from rice fields in Shanghai, China, and maintained on TN1 plants in a climate-controlled room at 26 ± 2 °C, 12 h/12 h light/dark cycle, and 80% relative humidity.

Individual test assay was carried out at seedling stage using at least six replicates of each cultivar or line as previously described[8,66]. Each seedling, about 5 weeks was infested with twelve second-instar BPH nymphs. Plant status were checked daily, and about 5–12 days later, the plants were scored as susceptible (dead) or resistant (alive) and photographed.

For the small population assay, about 40 plants of tested lines and the WT were planted in the mud in a plate for one month till about the third-leaf stage and fed to the BPH population inappropriately 10–15 first-instar nymphs per plant, and the plant status was surveyed daily. Plants were photographed, and the survival rates were calculated based on data from at least three repeats. The survival rate was calculated as follows, (the number of surviving plants / the total number of plants) × 100%.

For selection mechanism detection, each 2 germinated seeds of ACL1KO, *ACL1-D*, and ZH11 were evenly planted in the mud in a small pot with 10 repeats. About 6 weeks later, about 400 3-instar nymphs of BPH were collected and placed in the middle of the pot to let them scatter randomly. Each pot was covered by nylon mesh. The number of BPH on each plant was counted at 24 h, 48 h, and 72 h after infestation.

Each of the four plants of ACL1KO, *ACL1-D*, and ZH11 were planted in the mud in small pots with 10 repeats. About 6 weeks later, 50 2-instar nymphs of BPH were weighed to get an initial weight and then put to the plants after starvation for 2 h. Each line was arranged with 5 replicates, and another 5 replicates without feeding were simultaneously set up. After 7 days, the BPH was collected and weighed to calculate the weight gain. Meanwhile, the above-ground portions of both infested and uninfected plants were collected, dried, and weighed. Tolerance-related indicators refer to Sarao et al.[67]. Plant dry weight loss (mg) = dry weight of non-infested plant substrates dry weight of infested plant; Functional plant loss index (FPL, %) = (1- dry weight of infested plant/dry weight of uninfected plant) × 100; Plant dry weight loss to BPH dry weight produced = Plant dry weight loss/BPH weight gain.

Anatomical analysis

Anatomical sections of the GUS-stained tissues were carried out as described[68].

For manual sections, freshly collected flag leaves were manually cut into about 0.5 mm slices in the middle part as quickly as possible, and pictures were taken under NIKON D7000.

Histochemical GUS staining

GUS staining was carried out as previously described[69]. Photographs were taken under a stereo Leica M205FA.

Drought tolerance detection methods

For direct water cut-off, germinated seeds of the tested and control plants (about 40 plants for each line) were planted in parallel in the paddy soil in a 13 × 18 cm plastic box, grown in the phytotron for 4 weeks, then stopped watering until the plant withered (at about 5–11days), and re-watered again for 2–7 days to check the recovery status. The survival rates were calculated based on data from at least

three repeats. The survival rate was calculated as follows, (the number of surviving plants / the total number of plants) × 100%.

For 20% PEG6000 treatment, germinated seeds were planted in the plastic plate in the rice nutrient solution (Yoshida) (changed every 2 days) in the phytotron for 3 weeks. Treatment was carried out using 20% (w/v) PEG6000 solution solved in the rice nutrient solution until the plants were wilted (at about 6–20 days), and then replaced with the rice nutrient solution again (re-watering) for 2–7 days to check the recovery status. The survival rates were calculated based on data from at least three repeats. The survival rate was calculated as follows, (the number of surviving plants / the total number of plants) × 100%.

Scanning electron microscope (SEM) assay

The flag leaves, or the leaf sheaths was removed and quickly frozen in liquid nitrogen and then freeze-dried. The samples were observed by high-resolution field emission SEM Zeiss Merlin Compact.

Transmission electron microscopy (TEM) assay

The middle part of the second leaf of the two-week-old rice seedling was sampled, cut into small pieces (1-2 mm^2), and fixed in 2.5% (v/v) glutaraldehyde. Fixed leaves were embedded in Spurr's resin (SPI supplies) after dehydration through a graded alcohol series. Ultrathin sections (70 nm) were cut using the Leica Microsystem UC7 ultramicrotome and mounted on copper grids. Sectioned grids were stained with a saturated solution of uranyl acetate and lead citrate. The images were obtained at 80 kV with a Hitachi HT7700 transmission electron microscope. The cuticle thickness was measured by Image J software, and five biological replicates were measured for each sample.

GC-MS assay of the wax content

The leaves or sheaths of 6-week-old rice plants were cut and photographed immediately. Then Adobe Photoshop CS6 was used to calculate the leaf area of each sample. 3 ml chloroform that preheated to 60 °C was added into a 4 ml sample bottle, the clipped leaves or leaf sheaths were immersed in chloroform for 30 s, and 10 μg n-tetracosane (C24, TCI) was added as the internal standard. The bottles were dried using a nitrogen blower, the samples were dissolved in 100 μl pyridinium, and then 30 μl salinizing agent (BSTFA-TMCS (99:1), TCI) was added. The samples were taken out and cooled to room temperature after reaction for 1 h in a 70 °C incubator, and then transferred to a new sample vial. An Agilent 7890B GC system coupled with an Agilent 5977 MS was used. GC was performed on an HP-5MS column (Agilent, 30 m × 0.25 mm i.d., 0.25 μm film thickness, 5% phenyl methyl siloxane stationary phase). The carrier gas was helium (purity > 99.999%) at a constant flow rate of 1.0 ml/min. The GC oven temperature was programmed from an initial temperature of 50 °C for 2 min, ramped at 5 °C/min to 300 °C, and held at 300 °C for 15 min. The mass range was recorded from m/z 30 to m/z 350. Electron energy was kept at 70 eV, and the source temperature and the quads temperature were kept at 230 °C and 150 °C, respectively. The peaks were identified based on comparison with standards and the National Institute of Standards and Technology library (NIST, version 14). The peak areas were deduced by cumulative scoring, and the contents of each ingredient were deduced through comparison with C24. The final values were shown as unit leaf area. Wax load per unit leaf area was calculated based on the area of leaves used for wax extraction. Three replicates were carried out.

RNA isolation and Quantitative real-time RT–PCR (qRT–PCR) analysis

For verification of transgenic plants, seedlings were used. Total RNAs were extracted using TRIzol (Life Technologies, USA) and reverse transcribed using the First Strand cDNA Synthesis Kit (Toyobo). qRT–PCR was performed with the SYBR Green Real-time PCR Master Mix Kit (Toyobo), cDNA was synthesized from 1 μg of total RNA, and 1 μl of cDNA was used as a template for real-time analysis. The rice *actin* (LOC_Os03g50885) and *ubiquitin* (LOC_Os01g22490) were used as reference genes to normalize expression levels. Data from three biological repeats were collected, and the mean value with standard deviation was plotted.

RNA-seq analysis

The RNA was used to prepare libraries, which were sequenced on the BGISEQ-500 analyzer at BGI (Shenzhen). The clean reads were assembled de novo as contigs using the software of SOAPdenovo. All reads were then realigned onto contigs according to the paired-end reads overlap relationship, and all these contigs were joined into scaffold sequences. Finally, the intra-scaffold gaps were filled using the paired-end extracted reads. Those sequences that could not be extended in either direction were termed unigenes and for differentially expressed genes (DEG) analysis. The differentially expressed genes were analyzed for enrichment in KEGG Pathways. *P*-values were calculated using R's phyper function, followed by multiple test corrections. A pathway was considered significantly enriched in differentially expressed genes if its Qvalue was ≤ 0.05.

Luciferase complementation imaging assay (LCI)

The full-length cDNA of the *ACL1*, *ROC4*, and *ROC5* genes were cloned into the *Kpn*I and *Sal*I sites of pCAMBIA1300-CLuc. While the full-length cDNA of *ROC1-8*, *TPR1*, *TPR2*, *TPR3*, and the N-terminal domain of *TPR1*, *TPR2*, and *TPR3*, 525 bp of respectively cloned into the *Kpn*I and *Sal*I sites of pCAMBIA1300-NLuc. All the constructs for the test were transformed into A. tumefaciens GV3101 (pSoup-P19). Agrobacterium cells were re-suspended in infection solution (10 mM MES, 10 mM $MgCl_2$, and 200 μM acetosyringone) at OD600 = 1.0. The prepared suspensions were infiltrated into *N. benthamiana leaves*. After 2 days, the LUC signal was detected using a CCD camera and a 150 mg/mL luciferin solution.

For competitive LCI, the full-length cDNA of the *ROC4* and *ROC5* were cloned into the *Kpn*I and *Sal*I sites of pCAMBIA1300-CLuc and pCAMBIA1300-NLuc, respectively. The full-length cDNA of the *ACL1* gene was constructed into the *Xba*I and *Kpn*I sites of p1301-35S-Nos, and the p1301-35S-Nos empty vector was used as the control. The recombinant vector and the empty plasmid pGreenII 0800-LUC were transformed into *Agrobacterium* GV3101. The culture, injection, and signal detection processes were similar. The double luciferase reporter gene analysis system (Promega, Madison, WI) was used to determine the enzyme activity of LUC and REN. Relative LUC activity = LUC/REN. Five biological replicates were measured for each sample.

Co-IP Assay

The full-length cDNA of *ACL1* was fused with the FLAG tag, while the full-length cDNA of *ROC1-8* were respectively fused with the GFP tag. The recombinant and control vectors were transformed into *Agrobacterium* GV3101. The culture and infiltration processes were similar. Injected *N. benthamiana* leaves were harvested after 3 d and frozen in liquid nitrogen. Soluble proteins were extracted with NB1 buffer (50 mM Tris-MES (pH8.0), 500 mM sucrose, 1 mM $MgCl_2$, 10 mM EDTA, 5 mM DTT, 1 mM PMSF, Cocktail). Immunoprecipitation was performed with anti-FLAG-affinity beads (Sigma-Aldrich). Lysates were incubated with the prewashed beads for 3 h. Then the beads were washed 6 times and solubilized in an appropriate volume of extraction buffer. The fusion proteins were detected by immunoblotting using monoclonal anti-FLAG M2 antibody (Sigma-Aldrich) and monoclonal antibody anti-GFP (Huabio).

For the competitive Co-IP, the full-length cDNA of *ACL1* was fused with GFP, while the full-length cDNA of the *ROC1-8* encoding sequence was fused with FLAG and HA, respectively. The following processes were the same as the Co-IP processes, except that the fusion proteins were detected by immunoblotting using monoclonal anti-FLAG M2

antibody (Sigma-Aldrich), monoclonal antibody anti-GFP (Huabio) and HA tag Polyclonal antibody (Proteintech).

Bimolecular fluorescence complementation (BIFC)

The cDNA of the coding region of *ACL1* was cloned into the *Kpn*I and *Sal*I sites of pCAMBIA1300-35S-cYFP. Similarly, the cDNA sequences of the coding region of *ROC1-8* were cloned into the *Kpn*I and *Sal*I sites of pCAMBIA1300-35S-nYFP. The recombinant and control vectors were transformed into *Agrobacterium* GV3101, respectively. The culture and infiltration processes were usual. 2 days later, the signals of YFP and mCherry were detected using confocal microscopy (Leica TSC SP8 STED 3X).

Y2H

Y2H was carried out as described[70]. The encoding sequence of *ACL1*, *TPR1*, *TPR2*, *TPR3*, and the N-terminal domain of *TPR1*, *TPR2*, and *TPR3*, 525 bp of the coding region of each gene was cloned into the pGBKT7 vector. The encoding sequence of *ACL1* and *ROC1-8* was individually cloned into the pGADT7 vector.

Primer sequences

All the oligo sequences used in this study were listed in Supplementary Data 2.

Statistical analysis

All statistical analyses were performed using Graph Pad Prism 6 and Microsoft Excel 2016 software. All data were presented herein as the mean ± standard deviation and were compared using one-way ANOVA with two-sided Tukey's HSD test or two-tailed unpaired Student's t-test whenever appropriate. Significance was established with a *P*-value less than 0.05 compared to a reference sample. Statistical analysis and the number of biologically independent samples (n) for each experiment were described in the figure legends.

Reporting summary

Further information on research design is available in the Nature Portfolio Reporting Summary linked to this article.

Data availability

All data supporting the results of this study are available in the paper and in the Supplementary Information. The RNA-seq data generated in this study has been deposited in the NCBI SRA database under accession number PRJNA1110626. The raw MS data generated in this study have been deposited in the ProteomeXchange Consortium via the PRIDE partner repository under accession code PXD052228. Source data are provided in this paper.

References

1. Du, B. et al. Identification and characterization of Bph14, a gene conferring resistance to brown planthopper in rice. *Proc. Natl. Acad. Sci. USA* **106**, 22163–22168 (2009).
2. Cheng, X. et al. A rice lectin receptor-like kinase that is involved in innate immune responses also contributes to seed germination. *Plant J. Cell Mol. Biol.* **76**, 687–698 (2013).
3. Tamura, Y. et al. Map-based cloning and characterization of a brown planthopper resistance gene BPH26 from Oryza sativa L. ssp. indica cultivar ADR52. *Sci. Rep.* **4**, 5872 (2014).
4. Liu, Y. et al. A gene cluster encoding lectin receptor kinases confers broad-spectrum and durable insect resistance in rice. *Nat. Biotechnol.* **33**, 301–305 (2015).
5. Wang, Y. et al. Map-based cloning and characterization of BPH29, a B3 domain-containing recessive gene conferring brown planthopper resistance in rice. *J. Exp. Bot.* **66**, 6035–6045 (2015).
6. Ji, H. et al. Map-based cloning and characterization of the BPH18 gene from wild rice conferring resistance to brown planthopper (BPH) insect pest. *Sci. Rep.* **6**, 34376 (2016).
7. Ren, J. et al. Bph32, a novel gene encoding an unknown SCR domain-containing protein, confers resistance against the brown planthopper in rice. *Sci. Rep.* **6**, 37645 (2016).
8. Zhao, Y. et al. Allelic diversity in an NLR gene BPH9 enables rice to combat planthopper variation. *Proc. Natl. Acad. Sci. USA* **113**, 12850–12855 (2016).
9. Guo, J. et al. Bph6 encodes an exocyst-localized protein and confers broad resistance to planthoppers in rice. *Nat. Genet.* **50**, 297–306 (2018).
10. Shi, S. et al. Bph30 confers resistance to brown planthopper by fortifying sclerenchyma in rice leaf sheaths. *Mol. plant* **14**, 1714–1732 (2021).
11. Zhou, C. et al. Balancing selection and wild gene pool contribute to resistance in global rice germplasm against planthopper. *J. Integr. Plant Biol.* **63**, 1695–1711 (2021).
12. Ling, Y. & Weilin, Z. Genetic and biochemical mechanisms of rice resistance to planthopper. *Plant Cell Rep.* **35**, 1559–1572 (2016).
13. Hogenhout, S. A. & Bos, J. I. Effector proteins that modulate plant–insect interactions. *Curr. Opin. Plant Biol.* **14**, 422–428 (2011).
14. Guo, J. et al. A tripartite rheostat controls self-regulated host plant resistance to insects. *Nature* **618**, 799–807 (2023).
15. Hao, P. et al. Herbivore-induced callose deposition on the sieve plates of rice: an important mechanism for host resistance. *Plant Physiol.* **146**, 1810–1820 (2008).
16. Lewandowska, M., Keyl, A. & Feussner, I. Wax biosynthesis in response to danger: its regulation upon abiotic and biotic stress. *N. Phytol.* **227**, 698–713 (2020).
17. McFarlane, H. E. et al. Golgi- and trans-Golgi network-mediated vesicle trafficking is required for wax secretion from epidermal cells. *Plant Physiol.* **164**, 1250–1260 (2014).
18. Borisjuk, N., Hrmova, M. & Lopato, S. Transcriptional regulation of cuticle biosynthesis. *Biotechnol. Adv.* **32**, 526–540 (2014).
19. Seo, P. J. et al. The MYB96 transcription factor regulates cuticular wax biosynthesis under drought conditions in Arabidopsis. *Plant Cell* **23**, 1138–1152 (2011).
20. Zhu, X. & Xiong, L. Putative megaenzyme DWA1 plays essential roles in drought resistance by regulating stress-induced wax deposition in rice. *Proc. Natl. Acad. Sci. USA* **110**, 17790–17795 (2013).
21. Wang, Z. et al. The E3 Ligase DROUGHT HYPERSENSITIVE negatively regulates cuticular wax biosynthesis by promoting the degradation of transcription factor ROC4 in Rice. *Plant cell* **30**, 228–244 (2018).
22. Islam, M. A., Du, H., Ning, J., Ye, H. & Xiong, L. Characterization of Glossy1-homologous genes in rice involved in leaf wax accumulation and drought resistance. *Plant Mol. Biol.* **70**, 443–456 (2009).
23. Zhou, L. et al. Rice OsGL1-6 is involved in leaf cuticular wax accumulation and drought resistance. *PloS ONE* **8**, e65139 (2013).
24. Wang, Y. et al. An ethylene response factor OsWR1 responsive to drought stress transcriptionally activates wax synthesis related genes and increases wax production in rice. *Plant Mol. Biol.* **78**, 275–288 (2012).
25. Zhang, W. et al. Omics-based comparative transcriptional profiling of two contrasting rice genotypes during early infestation by small brown planthopper. *Int. J. Mol. Sci.* **16**, 28746–28764 (2015).
26. Fang, Y. & Xiong, L. General mechanisms of drought response and their application in drought resistance improvement in plants. *Cell. Mol. Life Sci.* **72**, 673–689 (2015).
27. Todaka, D., Shinozaki, K. & Yamaguchi-Shinozaki, K. Recent advances in the dissection of drought-stress regulatory networks and

strategies for development of drought-tolerant transgenic rice plants. *Front. Plant Sci.* **6**, 84 (2015).
28. Zhang, G. H., Xu, Q., Zhu, X. D., Qian, Q. & Xue, H. W. SHALLOT-LIKE1 is a KANADI transcription factor that modulates rice leaf rolling by regulating leaf abaxial cell development. *Plant Cell* **21**, 719–735 (2009).
29. Sirault, X. R., Condon, A. G., Wood, J. T., Farquhar, G. D. & Rebetzke, G. J. "Rolled-upness": phenotyping leaf rolling in cereals using computer vision and functional data analysis approaches. *Plant Methods* **11**, 52 (2015).
30. Li, L. et al. Overexpression of ACL1 (abaxially curled leaf 1) increased Bulliform cells and induced Abaxial curling of leaf blades in rice. *Mol. Plant* **3**, 807–817 (2010).
31. Xu, Y. et al. Overexpression of OsZHD1, a zinc finger homeodomain class homeobox transcription factor, induces abaxially curled and drooping leaf in rice. *Planta* **239**, 803–816 (2014).
32. Ohashi, Y. et al. Modulation of phospholipid signaling by GLABRA2 in root-hair pattern formation. *Science* **300**, 1427–1430 (2003).
33. Lin, Q. et al. GLABRA2 Directly Suppresses Basic Helix-Loop-Helix Transcription Factor Genes with Diverse Functions in Root Hair Development. *Plant Cell* **27**, 2894–2906 (2015).
34. Wu, R. & Citovsky, V. Adaptor proteins GIR1 and GIR2. II. Interaction with the co-repressor TOPLESS and promotion of histone deacetylation of target chromatin. *Biochem. Biophys. Res. Commun.* **488**, 609–613 (2017).
35. Zou, L. P. et al. Leaf rolling controlled by the homeodomain leucine zipper class IV gene Roc5 in rice. *Plant Physiol.* **156**, 1589–1602 (2011).
36. Xiang, J. J., Zhang, G. H., Qian, Q. & Xue, H. W. Semi-rolled leaf1 encodes a putative glycosylphosphatidylinositol-anchored protein and modulates rice leaf rolling by regulating the formation of bulliform cells. *Plant Physiol.* **159**, 1488–1500 (2012).
37. Zhao, S. Q., Hu, J., Guo, L. B., Qian, Q. & Xue, H. W. Rice leaf inclination2, a VIN3-like protein, regulates leaf angle through modulating cell division of the collar. *Cell Res.* **20**, 935–947 (2010).
38. Sun, J. et al. HD-ZIP IV gene Roc8 regulates the size of bulliform cells and lignin content in rice. *Plant Biotechnol. J.* **18**, 2559–2572 (2020).
39. Li, C. et al. OsLBD3-7 Overexpression Induced Adaxially Rolled Leaves in Rice. *PloS ONE* **11**, e0156413 (2016).
40. Shi, Z. et al. Over-expression of rice OsAGO7 gene induces upward curling of the leaf blade that enhanced erect-leaf habit. *Planta* **226**, 99–108 (2007).
41. Hu, J. et al. Identification and characterization of NARROW AND ROLLED LEAF 1, a novel gene regulating leaf morphology and plant architecture in rice. *Plant Mol. Biol.* **73**, 283–292 (2010).
42. Fang, L. et al. Rolling-leaf14 is a 2OG-Fe (II) oxygenase family protein that modulates rice leaf rolling by affecting secondary cell wall formation in leaves. *Plant Biotechnol. J.* **10**, 524–532 (2012).
43. Li, Y. Y. et al. Overexpression of OsHox32 Results in Pleiotropic Effects on Plant Type Architecture and Leaf Development in Rice. *Rice* **9**, 46 (2016).
44. Yang, S. Q. et al. REL2, A Gene Encoding An Unknown Function Protein which Contains DUF630 and DUF632 Domains Controls Leaf Rolling in Rice. *Rice* **9**, 37 (2016).
45. Ma, Y. et al. Overexpression of OsRRK1 Changes Leaf Morphology and Defense to Insect in Rice. *Front. Plant Sci.* **8**, 1783 (2017).
46. Wu, M. L. et al. NbCycB2 represses Nbwo activity via a negative feedback loop in tobacco trichome development. *J. Exp. Bot.* **71**, 1815–1827 (2020).
47. Gao, S. et al. The tomato B-type cyclin gene, SlCycB2, plays key roles in reproductive organ development, trichome initiation, terpenoids biosynthesis and Prodenia litura defense. *Plant Sci. Int. J. Exp. Plant Biol.* **262**, 103–114 (2017).
48. Brentassi, M. E., Corrales, C., Snape, J. W., Dixon, A. F. & Castro, A. M. Wheat antixenosis, antibiosis, and tolerance to infestation by Delphacodes kuscheli (Hemiptera: Delphacidae), a vector of "Mal de Rio Cuarto" in Argentina. *J. Economic Entomol.* **102**, 1801–1807 (2009).
49. Mair, A., Xu, S. L., Branon, T. C., Ting, A. Y. & Bergmann, D. C. Proximity labeling of protein complexes and cell-type-specific organellar proteomes in Arabidopsis enabled by TurboID. *ELife* **8**, e47864 (2019).
50. Zhang, Y. et al. TurboID-based proximity labeling reveals that UBR7 is a regulator of N NLR immune receptor-mediated immunity. *Nat. Commun.* **10**, 3252 (2019).
51. Chew, W., Hrmova, M. & Lopato, S. Role of Homeodomain leucine zipper (HD-Zip) IV transcription factors in plant development and plant protection from deleterious environmental factors. *Int. J. Mol. Sci.* **14**, 8122–8147 (2013).
52. Xu, Y. et al. Heterodimer formed by ROC8 and ROC5 modulates leaf rolling in rice. *Plant Biotechnol. J.* **19**, 2662–2672 (2021).
53. Ito, M. et al. Roles of rice GL2-type homeobox genes in epidermis differentiation. *Breed. Sci.* **53**, 245–253 (2003).
54. Plant, A. R., Larrieu, A. & Causier, B. Repressor for hire! The vital roles of TOPLESS-mediated transcriptional repression in plants. *N. Phytol.* **231**, 963–973 (2021).
55. Matschi, S. et al. Structure-function analysis of the maize bulliform cell cuticle and its potential role in dehydration and leaf rolling. *Plant Direct* **4**, e00282 (2020).
56. Seo, P. J. & Park, C. M. Cuticular wax biosynthesis as a way of inducing drought resistance. *Plant Signal. Behav.* **6**, 1043–1045 (2011).
57. Bi, H. et al. Wheat drought-responsive WXPL transcription factors regulate cuticle biosynthesis genes. *Plant Mol. Biol.* **94**, 15–32 (2017).
58. Wu, R. & Citovsky, V. Adaptor proteins GIR1 and GIR2. I. Interaction with the repressor GLABRA2 and regulation of root hair development. *Biochem. Biophys. Res. Commun.* **488**, 547–553 (2017).
59. Walker, A. R. et al. The TRANSPARENT TESTA GLABRA1 locus, which regulates trichome differentiation and anthocyanin biosynthesis in Arabidopsis, encodes a WD40 repeat protein. *Plant Cell* **11**, 1337–1350 (1999).
60. Khosla, A. et al. HD-Zip Proteins GL2 and HDG11 have redundant functions in arabidopsis trichomes, and GL2 activates a positive feedback loop via MYB23. *Plant Cell* **26**, 2184–2200 (2014).
61. Yang, C. et al. A regulatory gene induces trichome formation and embryo lethality in tomato. *Proc. Natl. Acad. Sci. USA* **108**, 11836–11841 (2011).
62. Wang, Z. et al. NtCycB2 negatively regulates tobacco glandular trichome formation, exudate accumulation, and aphid resistance. *Plant Mol. Biol.* **108**, 65–76 (2022).
63. Schrick, K., Ahmad, B. & Nguyen, H. V. HD-Zip IV transcription factors: Drivers of epidermal cell fate integrate metabolic signals. *Curr. Opin. Plant Biol.* **75**, 102417 (2023).
64. Bonaventure, G. Perception of insect feeding by plants. *Plant Biol.* **14**, 872–880 (2012).
65. Kim, T. W. et al. Mapping the signaling network of BIN2 kinase using TurboID-mediated biotin labeling and phosphoproteomics. *Plant Cell* **35**, 975–993 (2023).
66. Wang, Y., Li, H., Si, Y., Zhang, H. & Guo Miao, X. Microarray analysis of broad-spectrum resistance derived from an indica cultivar Rathu Heenati. *Planta* **235**, 829–840 (2012).
67. Sarao, P. S. & Bentur, J. S. Antixenosis and tolerance of rice genotypes against brown planthopper. *Rice Sci.* **23**, 96–103 (2016).

68. Wang, J. et al. Overexpression of Osta-siR2141 caused abnormal polarity establishment and retarded growth in rice. *J. Exp. Bot.* **61**, 1885–1895 (2010).
69. Dai, Z. et al. Modulation of plant architecture by the miR156f-OsSPL7-OsGH3.8 pathway in rice. *J. Exp. Bot.* **69**, 5117–5130 (2018).
70. Sun, B. et al. A novel transcriptional repressor complex MYB22-TOPLESS-HDAC1 promotes rice resistance to brown planthopper by repressing F3′H expression. *N. Phytol.* **239**, 720–738 (2023).

Acknowledgements

We would like to thank Dr. Ling Li from Shanghai Jiaotong University for the helpful discussion and Dr. Bo Du from Wuhan University for help with the CRISPR/CAS9 system. We would like to thank Prof. Tiegang Lu from the Chinese Academy of Agricultural Sciences for providing the *roc5* mutant. We would like to thank Prof. Mingyi Bai from Shandong University for providing the Gateway-compatible 35S-YFP-miniTurbo vector. We would like to thank Xiaoyan Gao, Zhiping Zhang, and Jiqin Li from our institute for assistance in electron microscopy, and Wenjuan Cai from our institute for assistance in confocal imaging. We thank PhD. Robert McKenzie from Liwen Bianji (Edanz) (www.liwenbianji.cn) for editing a draft of this manuscript. This research was supported by the National Natural Science Foundation of China (32072029 to Z.S., 31770280 to Z.S.) and a grant from the State Key Laboratory of Hybrid Rice (KF201805 to Z.S.).

Author contributions

X.M. and Z.S. conceived and supervised the project. X.M., Z.S., and Z.T. designed the experiments. Z.T., L.Z., and B.S. performed the experiments. H.L., X.L., and D.L. discussed the results and offered advice. Z.T., W.H., and S.W. analyzed the data. Z.S. wrote and revised the manuscript. X.M. revised the manuscript.

Competing interests

The authors declare no competing interests.

Additional information

Supplementary information The online version contains supplementary material available at https://doi.org/10.1038/s41467-024-52436-w.

Correspondence and requests for materials should be addressed to Xuexia Miao or Zhenying Shi.

Peer review information *Nature Communications* thanks the anonymous reviewer(s) for their contribution to the peer review of this work. A peer review file is available.